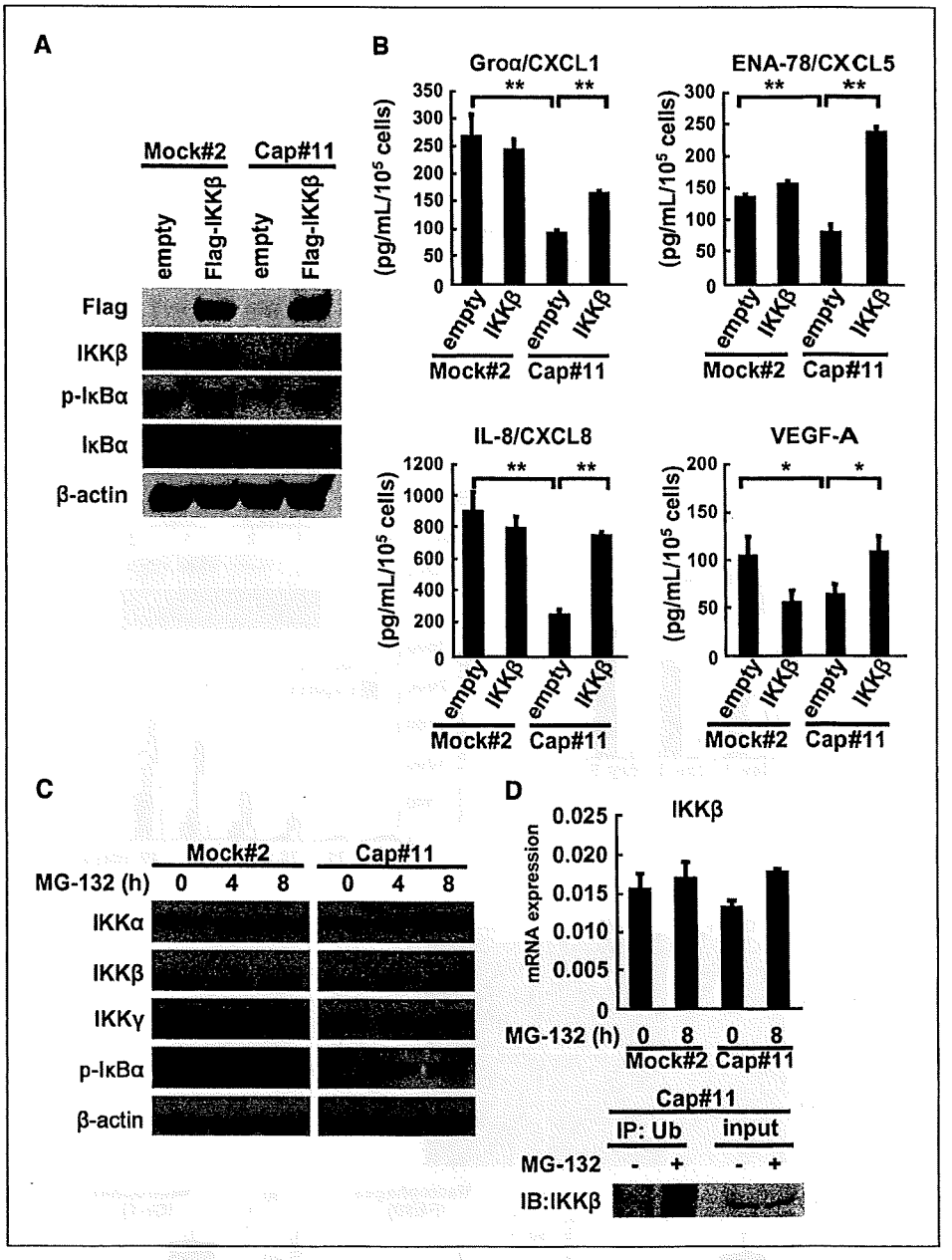

Figure 3. IKKβ overexpression restores the level of p-IκBα and expression of the CXC chemokines and VEGF-A. *A*, expression of the exogenous IKKβ gene and phosphorylation of IκBα in MIApaca-2 transfectants. NDRG1/Cap43 and mock transfectants were transiently transfected with the IKKβ expression vector. At 30 h after IKKβ transfection, the cells were again seeded and cultured for 18 h and then cultured in medium containing 2% serum for 24 h. *B*, ELISA assay analysis of Groα/CXCL1, ENA-78/CXCL5, IL-8/CXCL8, and VEGF-A protein levels in Mock#2 and Cap#11 that were transfected with the IKKβ expression vector. At 48 h after IKKβ transfection, the cells were cultured in medium containing 2% serum for 24 h. *Columns*, mean of three independent experiments; *bars*, SE. *, $P < 0.05$; **, $P < 0.01$ versus empty-transfected Cap#11 cells. *C*, Western blot analysis of IκBα phosphorylation and IKKα, IKKβ, and IKKγ expression in NDRG1/Cap43 and mock transfectants treated with MG-132 (10 μmol/L) in the presence of 2% serum for indicated time. *D*, quantitative real-time PCR analysis of IKKβ mRNA levels in NDRG1/Cap43 and mock transfectants treated with MG-132 (10 μmol/L) in the presence of 2% serum for the indicated time. *Columns*, mean of three independent experiments; *bars*, SE (*top*). Cells were treated with or without MG-132 (10 μmol/L) for 8 h before lysis. Immunoprecipitation was done with anti-ubiquitin (*Ub*) antibody and immunoblotting was with anti-IKKβ antibody (*bottom*).

(Fig. 3*D*, *top*). We further examined whether IKKβ was ubiquitinated or not in the presence of MG-132. As shown in Fig. 3*D* (*bottom*), ubiquitination of IKKβ was shown in Cap#11 cells, suggesting that a proteasomal degradation plays a role in down-regulation of IKKβ in the NDRG/Cap43-expressing cells.

NDRG1/Cap43 suppresses infiltration of inflammatory cells, expression of angiogenesis-related factors, tumor growth, and tumor angiogenesis. Consistent with our previous study (5), there was no difference in growth rates among Mock#2 and Cap#11 cells in culture (Fig. 4*A*). By contrast, tumor growth of Cap#11 was markedly reduced in comparison with Mock#2 in a subcutaneous mouse xenograft model (Fig. 4*B*, *bottom*). Immunoblotting analysis showed that NDRG1/Cap43 protein was consistently and highly expressed in Cap#11 tumors on day 49 after inoculation compared with Mock#2 tumors (Fig. 4*B*, *top*).

NDRG1/Cap43 was found to reduce the expression of chemokines and growth factors that function in chemotaxis of monocytes/macrophages and neutrophils (Fig. 1*B*; Supplementary Fig. S1). Mock#2 and Cap#11 tumor sections were further analyzed by immunohistochemistry for expression of microvessels (CD31), macrophages (F4/80), and neutrophils (Gr-1; Fig. 4*C*, *top*). MVD staining showed a markedly higher number of tumor neovessels in Mock#2 tumors than in Cap#11 tumors on day 49 after implantation (Fig. 4*C*, *bottom*). There appeared to be much lower infiltration of F4/80-positive macrophages and also Gr-1-positive infiltrating neutrophils in the stroma of Cap#11 tumors compared with that of Mock#2 tumors (Fig. 4*C*, *bottom*). NDRG1/Cap43 expression was thus closely associated with decreased MVD and also with a decreased number of infiltrating macrophages and neutrophils in mouse xenograft tumors. Expression of IL-8/CXCL8 and

VEGF-A was significantly reduced in Cap#11 tumors compared with Mock#2 tumors (Fig. 4*D*), suggesting that reduced expression of such chemokines and growth factors was continuously maintained during tumor growth in this mouse xenograft model.

Association of NDRG1/Cap43 expression level with infiltrating inflammatory cells in tumors of pancreatic cancer patients. Expression of NDRG1/Cap43 was previously shown to be inversely correlated with MVD in the tumors of patients with pancreatic cancer (5). Based on the expression level of NDRG1/Cap43 in resected specimens from 37 patients with pancreatic ductal adenocarcinoma, we divided them into two groups: NDRG1/Cap43 positive (n = 18) and NDRG1/Cap43 negative (n = 19). Supplementary Table S3 shows the association between NDRG1/Cap43 expression and clinicopathologic variables such as age, gender, depth of invasion, lymph node metastasis, and pathologic stage in patients with pancreatic ductal adenocarcinoma. High NDRG1/Cap43 expression was significantly correlated with invasion depth (Supplementary Table S3).

In the human tumor stroma, some cases showed a lower number of infiltrating $CD68^+$ macrophages/monocytes in NDRG1/Cap43-positive pancreatic cancer (Fig. 5*A*, *a* and *b*), whereas others showed a higher number of infiltrating $CD68^+$ macrophages/monocytes in NDRG1/Cap43-negative pancreatic cancer (Fig. 5*A*, *c* and *d*). Quantitative analysis indicated that the number of infiltrating macrophages/monocytes was relatively higher in patients with NDRG1/Cap43-negative tumors than in those with NDRG1/Cap43-positive tumors (Fig. 5*A*, *right*), the mean number of infiltrating macrophages/monocytes being 97.5 and 62.3, respectively. However, similar numbers of infiltrating neutrophils were observed in the tumor stroma of patients with NDRG1/Cap43-positive and

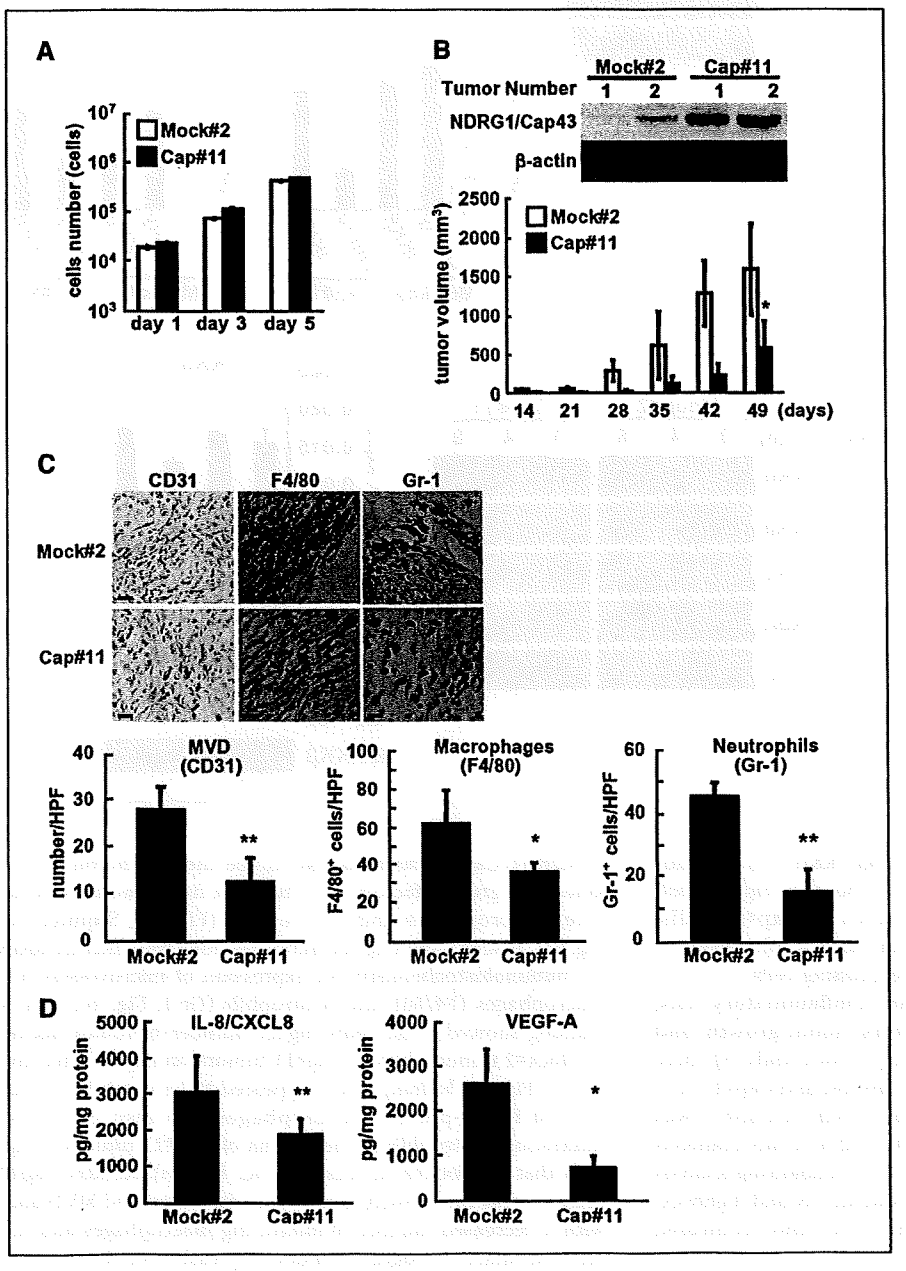

Figure 4. NDRG1/Cap43 represses MVD and the number of infiltrating macrophages or neutrophils in mouse subcutaneous tumors. *A*, comparison of cell proliferation in MIApaca-2 transfectant cells (Mock#2 and Cap#11). Cells were seeded on day 0 at 1.0×10^4 per well and cultured in DMEM with 10% serum. Cell growth was measured on days 1, 3, and 5. *Columns*, mean of three independent experiments; *bars*, SE. *B*, Western blot analysis of NDRG1/Cap43 expression in tumors comprising Mock#2 or Cap#11 cells on day 49 (*top*). *Columns*, mean tumor volumes; *bars*, SE. Tumor volumes were determined every week after tumor implantation (n = 5 or 6; *bottom*). *C*, immunohistochemical analysis. Representative photographs of tumor sections stained with the anti-CD31, anti-F4/80, and anti-Gr-1 antibodies from Mock#2 and Cap#11 xenografts on day 49. *Bar*, 25 μm (*top*). Mean MVD for tumor sections from Mock#2 and Cap#11 xenografts on day 49 was determined by counting the number of $CD31^+$ vessels in the tumors. Mean numbers of infiltrating macrophages and neutrophils in tumor sections from Mock#2 and Cap#11 xenografts on day 49 were determined by counting the intensity of F4/80- or Gr-1-positive cells in the tumor stroma. *Columns*, mean; *bars*, SE (n = 5; *bottom*). *HPF*, high-power field. *D*, ELISA assay analysis of human IL-8/CXCL8 and VEGF-A protein levels in Mock#2 and Cap#11 tumors. *Columns*, mean; *bars*, SE (n = 4). *, $P < 0.05$; **, $P < 0.01$ versus Mock#2 tumors.

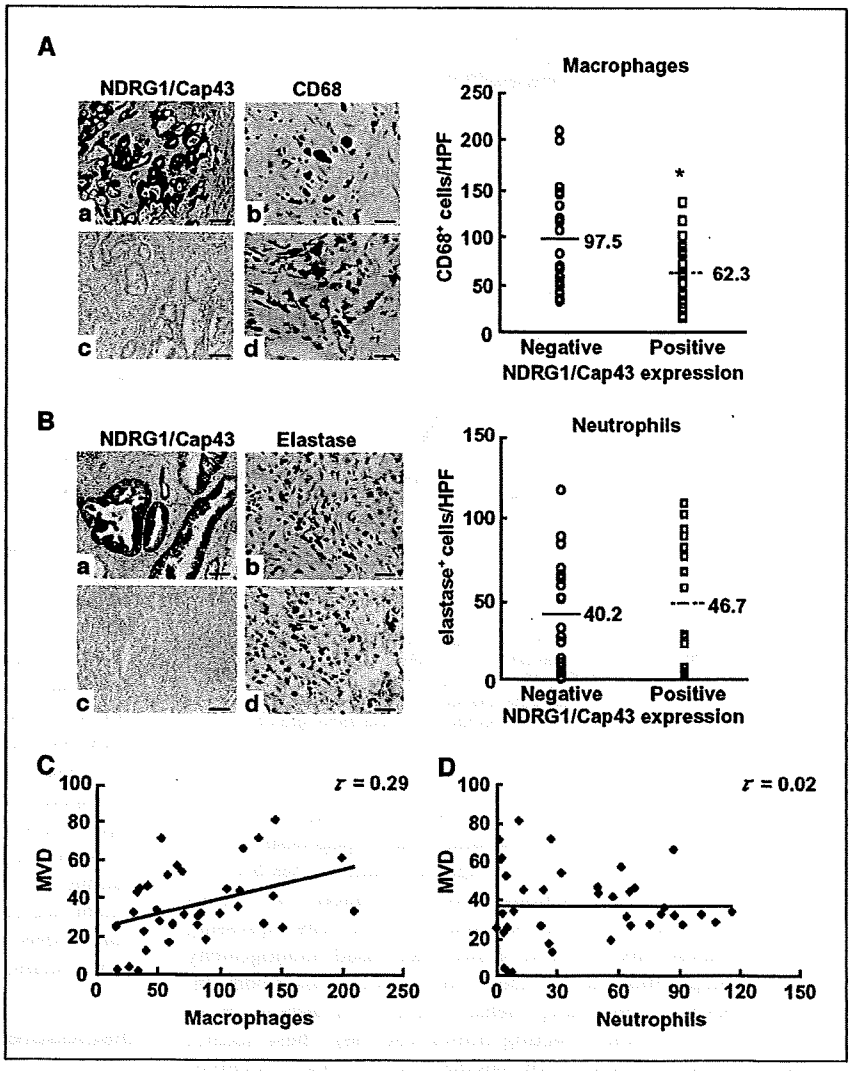

Figure 5. NDRG1/Cap43 expression levels and numbers of infiltrating inflammatory cells in human pancreatic cancer. *A*, immunohistochemical analysis of macrophages in tumor stroma using the anti-NDRG1/Cap43 antibody and anti-CD68 antibody. Representative photographs showing low infiltration of macrophages in NDRG1/Cap43-positive specimens (*a* and *b*). Representative photographs showing high infiltration of macrophages in NDRG1/Cap43-negative specimens (*c* and *d*). *Bar*, 50 μm (*a* and *c*) and 25 μm (*b* and *d*). Correlation between NDRG1/Cap43 expression levels and numbers of infiltrating macrophages. Mean number of infiltrating macrophages was 97.5 in NDRG1/Cap43-negative specimens ($n = 19$) and 62.3 in NDRG1/Cap43-positive specimens ($n = 18$; *right*). *, $P < 0.05$. *B*, immunohistochemical analysis of neutrophils in tumor stroma using an anti-NDRG1/Cap43 antibody and anti-elastase antibody. Representative photographs of neutrophils infiltration in NDRG1/Cap43-positive specimens (*a* and *b*) and NDRG1/Cap43-negative specimens (*c* and *d*). Correlation between NDRG1/Cap43 expression level and number of infiltrating neutrophils. Mean number of infiltrating neutrophils was 40.2 in NDRG1/Cap43-negative specimens and 46.7 in NDRG1/Cap43-positive specimens (*right*). *C* and *D*, correlation between MVD and number of infiltrating macrophages or neutrophils in patients with pancreatic ductal adenocarcinoma ($n = 37$). $r = 0.29$ and 0.02, Kendall correlation coefficient.

NDRG1/Cap43-negative pancreatic cancer (Fig. 5*B*). Quantitative analysis showed that the mean number of infiltrating neutrophils was 40.2 in NDRG1/Cap43-negative specimens and 46.7 in NDRG1/Cap43-positive specimens, with no significant difference (Fig. 5*B*, *right*).

Our previous study showed that NDRG1/Cap43 expression levels were inversely correlated with MVD (5). Therefore, we further examined whether infiltration of macrophages/monocytes and neutrophils was associated with MVD in patients with NDRG1/Cap43-positive and NDRG1/Cap43-negative pancreatic cancer ($n = 37$). The number of infiltrating macrophages/monocytes was positively correlated with MVD (Fig. 5*C*; $P < 0.05$). However, there was no correlation between the number of infiltrating neutrophils and the MVD (Fig. 5*D*).

Discussion

We reported previously that NDRG1/Cap43 overexpression suppressed the expression of VEGF-A, IL-8/CXCL8, and matrix metalloproteinase-9 in pancreatic cancer cells (5). In the present study, we showed that NDRG1/Cap43 down-regulated the expression of several other genes, including chemoattractants for inflammatory cells. We also observed that decreased expression of IL-8/CXCL8 and VEGF-A in mouse tumors was associated with high expression of NDRG1/Cap43. These chemoattractants down-regulated by NDRG1/Cap43 had chemotactic effects on monocytes/macrophages and neutrophils. Our results showed that overexpression of NDRG1/Cap43 resulted in marked decrease in infiltration of macrophages and neutrophils in xenograft models.

One critical step in progression from a benign to a malignant state is angiogenesis. Infiltration of activated fibroblasts (21), macrophages/monocytes (22), and neutrophils (23) is expected to play a key role in the angiogenic switch of cancer (23–25). From our laboratory, we have also reported that infiltration of macrophages in the tumor stroma markedly promoted angiogenesis through the secretion of various proangiogenic cytokines and extracellular matrix-degrading proteases (18, 26–29). Groα/CXCL1, ENA-78/CXCL5, and IL-8/CXCL8 play an important role in tumor-associated angiogenesis and tumorigenesis in cancers of the kidney, pancreas, head and neck, and lung (30–33). Also, expression of CXC chemokines and VEGF-A would thus be expected to be closely involved in NDRG1/Cap43-induced suppression of tumor angiogenesis (Fig. 6). However, it is important to elucidate in more detail the underlying mechanism by which cytokines and growth

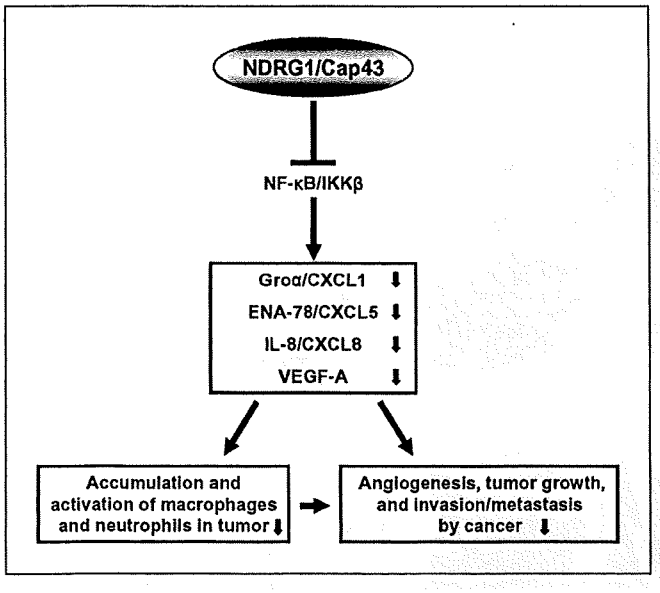

Figure 6. NDRG1/Cap43 plays a critical role as an antiangiogenic regulator through modulation of the tumor microenvironment in pancreatic cancer. NDRG1/Cap43 attenuates activation of the NF-κB/IKKβ signaling, resulting in decreased expression of CXC chemokines (Groα/CXCL1, ENA-78/CXCL5, and IL-8/CXCL8) and VEGF-A. NDRG1/Cap43 might thus remodel the tumor microenvironment by affecting the accumulation of inflammatory cells (macrophages and neutrophils), tumor angiogenesis, and tumor growth.

factors are directly involved in the NDRG1/Cap43-dependent suppression of inflammatory cell infiltration and angiogenesis.

Constitutive activation of NF-κB signaling pathway has been reported in many cancers, including pancreatic cancer (34). Fujioka and colleagues reported that pancreatic cancer cells expressing phosphorylation-defective IκBα showed decreased tumorigenicity in an orthotopic nude mouse model (35). In this mouse model, deletion of IKKβ in intestinal epithelial cells led to a decrease in tumor incidence without affecting tumor size (36). These studies suggested that the IKKβ-NF-κB signaling pathway plays an important role in tumor development.

In our present study, NDRG1/Cap43 reduced the expression of p-IκBα and its upstream regulator IKKβ in pancreatic cancer cells. However, we found no apparent phosphorylation of IKKα and IKKβ in NDRG1/Cap43 and mock transfectants under 2% serum condition (data not shown), suggesting that decreased expression of IKKβ is responsible for the loss of p-IκBα in NDRG1/Cap43 transfectants. The loss of p-IκBα results in reduction of both nuclear translocation of p65 and p50 and their binding to the NF-κB motif. NDRG1/Cap43-induced suppression of IKKβ was almost completely restored by a proteasome inhibitor. Introduction of an exogenous IKKβ gene was able to restore IκBα phosphorylation and expression of Groα/CXCL1, ENA-78/CXCL5, IL-8/CXCL8, and VEGF-A in NDRG1/Cap43 transfectants. In this study, we also found ubiquitination of IKKβ in NDRG1/Cap43 transfectant. A relevant study by May and colleagues showed that a ubiquitin-like domain of IKKβ is required for its functional activation (20). Taken together, the IKKβ-NF-κB pathway is expected to be attenuated by NDRG1/Cap43, resulting in decreased expression of angiogenesis and chemotaxis-related factors (see Fig. 6).

In various solid human tumors, an increase in the number of infiltrating tumor-associated macrophages has been shown to be closely associated with not only prognosis but also tumor angiogenesis (29, 37, 38). In our present study, a significantly decreased number of macrophages was also observed in clinical specimens of pancreatic cancer showing relatively higher NDRG1/Cap43 expression. The number of infiltrating macrophages was correlated with neovascularization in patients with pancreatic cancer. By contrast, we did not observe any significant difference in the number of infiltrating neutrophils between human pancreatic cancers showing low and high expression of NDRG1/Cap43. As shown in Fig. 4, in mouse xenograft models, chemotaxis of neutrophils and macrophages/monocytes was suppressed in Cap#11 xenograft. By contrast, in clinical specimens of pancreatic cancer, infiltration of macrophages, but not neutrophils, was significantly associated with higher NDRG1/Cap43 expression. It remains unclear why NDRG1/Cap43 has no effect on the infiltration of neutrophils in clinical specimens of pancreatic cancer, and this question requires further study, focusing particularly on pancreatic cancer at earlier stages.

In conclusion, this study has shown that NDRG1/Cap43 decreases the expression of IKKβ and the NF-κB signaling pathway. As a consequence, NDRG1/Cap43 decreases the expression of chemoattractants such as CXC chemokines and VEGF-A for inflammatory cells, leading to a marked decrease in the recruitment of macrophages and/or neutrophils, along with angiogenesis suppression, in xenograft models. Therefore, NDRG1/Cap43 could be a potent biomarker for modulation of the tumor stroma in pancreatic cancer.

Disclosure of Potential Conflicts of Interest

No potential conflicts of interest were disclosed.

Acknowledgments

Received 12/22/08; revised 3/12/09; accepted 4/17/09; published OnlineFirst 6/2/09.

Grant support: Grants-in-aid for Scientific Research in Priority Areas of Cancer from the Ministry of Education Culture, Sports Science, and Technology of Japan (M. Ono), Third-Term Comprehensive Control Research for Cancer from the Ministry of Health, Labor and Welfare, Japan (M. Kuwano), and Formation of Innovation Center for Fusion of Advanced Technologies, Kyushu University (M. Ono and M. Kuwano), and JSPS-Asia Core Program (M. Ono).

The costs of publication of this article were defrayed in part by the payment of page charges. This article must therefore be hereby marked *advertisement* in accordance with 18 U.S.C. Section 1734 solely to indicate this fact.

We thank Drs. K. Matsuo, T. Utsugi (Hanno Research Center for Taiho Parmaceutical), Y. Maruyama, and Y. Basaki (Kyushu University) for fruitful discussions.

References

1. Berger JC, Vander Griend DJ, Robinson VL, Hickson JA, Rinker-Schaeffer CW. Metastasis suppressor genes: from gene identification to protein function and regulation. Cancer Biol Ther 2005;4:805–12.
2. Kovacevic Z, Richardson DR. The metastasis suppressor, Ndrg-1: a new ally in the fight against cancer. Carcinogenesis 2006;27:2355–66.
3. Guan RJ, Ford HL, Fu Y, Li Y, Shaw LM, Pardee AB. Drg-1 as a differentiation-related, putative metastatic suppressor gene in human colon cancer. Cancer Res 2002;60:749–55.
4. Bandyopadhyay S, Pai SK, Gross SC, et al. The Drg-1 gene suppresses tumor metastasis in prostate cancer. Cancer Res 2003;63:1731–6.
5. Maruyama Y, Ono M, Kawahara A, et al. Tumor growth suppression in pancreatic cancer by a putative metastasis suppressor gene Cap43/NDRG1/Drg-1 through modulation of angiogenesis. Cancer Res 2006; 66:6233–42.
6. Fotovati A, Fujii T, Yamaguchi M, et al. 17β-Estradiol induces down-regulation of Cap43/NDRG1/Drg-1, a putative differentiation-related and metastasis suppressor gene, in human breast cancer cells. Clin Cancer Res 2006;12:3010–8.
7. Bandyopadhyay S, Pai SK, Hirota S, et al. Role of the

putative tumor metastasis suppressor gene Drg-1 in breast cancer progression. Oncogene 2004;23:5675–81.

8. Ando T, Ishiguro H, Kimura M, et al. Decreased expression of NDRG1 is correlated with tumor progression and poor prognosis in patients with esophageal squamous cell carcinoma. Dis Esophagus 2006;19: 454–8.
9. Koshiji M, Kumamoto K, Morimura K, et al. Correlation of N-myc downstream-regulated gene 1 expression with clinical outcomes of colorectal cancer patients of different race/ethnicity. World J Gastroenterol 2007;213: 2803–10.
10. Fukahori S, Yano H, Tsuneoka M, et al. Immunohistochemical expressions of Cap43 and Mina53 proteins in neuroblastoma. J Pediatr Surg 2007;42:1831–40.
11. Chua MS, Sun H, Cheung ST, et al. Overexpression of NDRG1 is an indicator of poor prognosis in hepatocellular carcinoma. Mod Pathol 2007;20:76–83.
12. Nishio S, Ushijima K, Tsuda N, et al. Cap43/NDRG1/Drg-1 is a molecular target for angiogenesis and a prognostic indicator in cervical adenocarcinoma. Cancer Lett 2008;264:36–43.
13. Nishie A, Masuda K, Otsubo M, et al. High expression of the Cap43 gene in infiltrating macrophages of human renal cell carcinomas. Clin Cancer Res 2001;7:2145–51.
14. Masuda K, Ono M, Okamoto M, et al. Downregulation of Cap43 gene by von Hippel-Lindau tumor suppressor protein in human renal cancer cells. Int J Cancer 2003;105:803–10.
15. Basaki Y, Hosoi F, Oda Y, et al. Akt-dependent nuclear localization of Y-box-binding protein 1 in acquisition of malignant characteristics by human ovarian cancer cells. Oncogene 2006;26:2736–46.
16. Izumi H, Ise T, Murakami T, et al. Structural and functional characterization of two human V-ATPase subunit gene promoters. Biochim Biophys Acta 2003; 1628:97–104.
17. Ono M, Hirata A, Kometani T, et al. Sensitivity to gefitinib (Iressa, ZD1839) in non-small cell lung cancer cell lines correlates with dependence on the epidermal growth factor (EGF) receptor/extracellular signal-regulated kinase 1/2 and EGF receptor/Akt pathway for proliferation. Mol Cancer Ther 2004;3:465–72.
18. Nakao S, Kuwano T, Tsutsumi-Miyahara C, et al. Infiltration of COX-2-expressing macrophages is a prerequisite for IL-1β-induced neovascularization and tumor growth. J Clin Invest 2005;115:2979–91.
19. Maeda S, Omata M. Inflammation and cancer: role of nuclear factor-κB activation. Cancer Sci 2008;99:836–42.
20. May MJ, Larsen SE, Shim JH, Madge LA, Ghosh S. A novel ubiquitin-like domain in IκB kinase β is required for functional activity of the kinase. J Biol Chem 2004; 279:45528–39.
21. Orimo A, Gupta PB, Sgroi DC, et al. Stromal fibroblasts present in invasive human breast carcinomas promote tumor growth and angiogenesis through elevated SDF-1/CXCL12 secretion. Cell 2005;121:335–48.
22. Condeelis J, Pollard JW. Macrophages: obligate partners for tumor cell migration, invasion, and metastasis. Cell 2006;124:263–6.
23. Nozawa H, Chiu C, Hanahan D. Infiltrating neutrophils mediate the initial angiogenic switch in a mouse model of multistage carcinogenesis. Proc Natl Acad Sci U S A 2006;103:12493–8.
24. Mahadevan D, Von Hoff DD. Tumor-stroma interactions in pancreatic ductal adenocarcinoma. Mol Cancer Ther 2007;6:1186–97.
25. Ardi VC, Kupriyanova TA, Deryugina EI, Quigley JP. Human neutrophils uniquely release TIMP-free MMP-9 to provide a potent catalytic stimulator of angiogenesis. Proc Natl Acad Sci U S A 2007;104:20262–7.
26. Torisu H, Ono M, Kiryu H, et al. Macrophage infiltration correlates with tumor stage and angiogenesis in human malignant melanoma: possible involvement of TNFα and IL-1α. Int J Cancer 2000;85:182–8.
27. Kuwano T, Nakao S, Yamamoto H, et al. Cyclooxygenase 2 is a key enzyme for inflammatory cytokine-induced angiogenesis. FASEB J 2004;18:300–10.
28. Kimura YN, Watari K, Fotovati A, et al. Inflammatory stimuli from macrophages and cancer cells synergistically promote tumor growth and angiogenesis. Cancer Sci 2007;98:2009–18.
29. Ono M. Molecular links between tumor angiogenesis and inflammation: inflammatory stimuli of macrophages and cancer cells as targets for therapeutic strategy. Cancer Sci 2008;99:1501–6.
30. Pöld M, Zhu LX, Sharma S, et al. Cyclooxygenase-2-dependent expression of angiogenic CXC chemokines ENA-78/CXC ligand (CXCL) 5 and interleukin-8/CXCL8 in human non-small cell lung cancer. Cancer Res 2004; 64:1853–60.
31. Mestas J, Burdick MD, Reckamp K, Pantuck A, Figlin RA, Strieter RM. The role of CXCR2/CXCR2 ligand biological axis in renal cell carcinoma. J Immunol 2005;175: 5351–7.
32. Wente MN, Keane MP, Burdick MD, et al. Blockade of the chemokine receptor CXCR2 inhibits pancreatic cancer cell-induced angiogenesis. Cancer Lett 2006; 241:221–7.
33. Miyazaki H, Patel V, Wang H, Edmunds RK, Gutkind JS, Yeudall WA. Down-regulation of CXCL5 inhibits squamous carcinogenesis. Cancer Res 2006;66:4279–84.
34. Zhang Z, Rigas B. NF-κB, inflammation and pancreatic carcinogenesis: NF-κB as a chemoprevention target. Int J Oncol 2006;29:185–92.
35. Fujioka S, Sclabas GM, Schmidt C, et al. Inhibition of constitutive NF-κB activity by IκBαM suppresses tumorigenesis. Oncogene 2003;22:1365–70.
36. Greten FR, Eckmann L, Greten TF, et al. IKKβ links inflammation and tumorigenesis in a mouse model of colitis-associated cancer. Cell 2004;118:285–96.
37. Bingle L, Brown NJ, Lewis CE. The role of tumor-associated macrophages in tumor progression: implications for new anticancer therapies. J Pathol 2002;196: 254–65.
38. Chen JJ, Yao PL, Yuan A, et al. Up-regulation of tumor interleukin-8 expression by infiltrating macrophages: its correlation with tumor angiogenesis and patient survival in non-small cell lung cancer. Clin Cancer Res 2003;9: 729–37.

Overexpression of Class III β-Tubulin Predicts Good Response to Taxane-Based Chemotherapy in Ovarian Clear Cell Adenocarcinoma

Daisuke Aoki,[1] Yoshinao Oda,[3] Satoshi Hattori,[8] Ken-ichi Taguchi,[7] Yoshihiro Ohishi,[3] Yuji Basaki,[5,6] Shinji Oie,[2] Nao Suzuki,[10] Suminori Kono,[4] Masazumi Tsuneyoshi,[3] Mayumi Ono,[5,6] Takashi Yanagawa,[8] and Michihiko Kuwano[6,9]

Abstract

Purpose: Of the various microtubule-associated molecules, β-tubulin III has been reported to be closely associated with the therapeutic efficacy of taxane-based chemotherapy against ovarian cancer. Stathmin and microtubule-associated protein 4 (MAP4) have been reported to play an important role in microtubule stabilization. In this study, we investigated whether expression of these microtubule-associated factors affects the therapeutic efficacy of taxane-based chemotherapy in ovarian clear cell adenocarcinoma.

Experimental Design: Drug sensitivity of paclitaxel or cisplatin was assessed in ovarian cancer cell lines treated with small interfering RNA of tubulin isoforms, MAP4, and stathmin. We examined 94 surgically resected ovarian clear cell adenocarcinoma specimens from patients treated with taxane-containing regimens ($n = 44$) and with taxane-free regimens ($n = 50$), using immunohistochemistry to detect expression of β-tubulin III, stathmin, and MAP4.

Results: Knockdown of β-tubulin III and IV specifically conferred drug resistance to paclitaxel in one ovarian cancer cell line, but not to other molecules. Estimated overall survival revealed a significant synergistic effect between taxane and β-tubulin III in patients with ovarian clear cell adenocarcinoma. Of three microtubule-related molecules, among the taxane-based chemotherapy group, cases with higher β-tubulin III expression were associated with a significantly more favorable prognosis compared with those having lower β-tubulin III expression. By contrast, there was no statistical significance in the synergistic relationships between stathmin and taxane or between MAP4 and taxane.

Conclusions: Taxane-based chemotherapy was effective for patients with ovarian clear cell adenocarcinomas who were positive for β-tubulin III but not for those who were negative for these proteins.

Microtubules are the principal target of a large and diverse group of natural-product anticancer therapeutic drugs, particularly of two major classes of antimicrotubule agents: the vinca alkaloids and the taxanes (1). Microtubules are composed of polymers of heterodimers that consist of two closely related polypeptides, α-tubulin and β-tubulin, which in turn contain α- or β-subunits and at least six isotypes encoded by different genes. Isotype composition influences the intrinsic dynamics of microtubules, and the sensitivity of microtubules to depolymerizing and polymerizing agents is related to the composition of tubulin isotypes or microtubule-associated proteins (MAP; ref. 2). MAPs, important components of the tubulin and microtubule system, can bind to the microtubule wall and stabilize microtubules (3). MAP2 and MAP-τ are abundantly expressed in mature neurons, and MAP4 is ubiquitously expressed in both proliferating and differentiated cells (4). Stathmin is also the founding member of the microtubule-destabilizing family of proteins, which regulate the dynamics of microtubule polymerization and depolymerization. Stathmin is expressed at high levels in a variety of human cancers

Authors' Affiliations: [1]Department of Obstetrics and Gynecology, School of Medicine, Keio University, and [2]Personalized Medicine Research Laboratory, Taiho Pharmaceutical Co Ltd., Tokyo, Japan; Departments of [3]Anatomic Pathology and [4]Preventive Medicine, Graduate School of Medical Sciences, [5]Department of Pharmaceutical Oncology, Graduate School of Pharmaceutical Sciences, and [6]Innovation Center for Medical Redox Navigation, Kyushu University, and [7]Kyushu National Cancer Center, Fukuoka, Japan; [8]Biostatistics Center and [9]Research Center for Innovative Cancer Therapy, Kurume University, Kurume City, Japan; and [10]Department of Obstetrics and Gynecology, School of Medicine, Saint. Marianna University, Kawasaki, Japan

Received 8/16/08; revised 10/31/08; accepted 11/7/08.

Grant support: Grant-in-Aid for Scientific Research on Priority Areas, Cancer, from the Ministry of Education, Culture, Sports, Science and Technology of Japan (M. Ono), and by the Third Term Comprehensive Control Research for Cancer from the Ministry of Health, Labor and Welfare, Japan (M. Kuwano). This study was also supported, in part, by the Formation of Innovation Center for Fusion of Advanced Technologies, Kyushu University, Japan (M. Ono, Y. Basaki, and M. Kuwano).

The costs of publication of this article were defrayed in part by the payment of page charges. This article must therefore be hereby marked *advertisement* in accordance with 18 U.S.C. Section 1734 solely to indicate this fact.

Note: Supplementary data for this article are available at Clinical Cancer Research Online (http://clincancerres.aacrjournals.org/).

D. Aoki, Y. Oda, S. Hattori, K. Taguchi, Y. Ohishi, and Y. Basaki contributed equally to this work.

Requests for reprints: Daisuke Aoki, Department of Obstetrics and Gynecology, School of Medicine, Keio University, 35 Shinanomachi, Shinjuku-ku, Tokyo 160-8582, Japan. Phone: 81-3-3353-1211; Fax: 81-3-3226-1667; E-mail: aoki@sc.itc.keio.ac.jp.

doi:10.1158/1078-0432.CCR-08-1274

Translational Relevance

It has been reported that β-tubulin III, one of microtubule-associated molecules, was expected to be a useful biomarker for the clinical efficacy of taxane-based chemotherapy against human ovarian cancer. These studies have been conducted in serous adenocarcinoma of ovarian cancer. Previous reports show, however, that ovarian clear cell adenocarcinoma constituted about 20% of ovarian adenocarcinoma in Japan, although only 2% to 5% of cases of ovarian cancer worldwide were clear cell adenocarcinoma. Clear cell adenocarcinoma, which is a rare variant in western counties, has been recognized as a chemoresistant phenotype compared with serous adenocarcinoma, which is the most widespread ovarian cancer. This study aimed to identify a predictive marker for the clinical efficacy of taxane-based chemotherapy against ovarian clear cell adenocarcinoma. In this study, we found that a taxane-based regimen was effective for patients with ovarian clear cell adenocarcinomas who were positive for stathmin or β-tubulin III.

and also plays a role in altered drug sensitivity in human cancer cells, including ovarian cancer cells (5, 6).

The antitumor drug taxane stabilizes microtubules and reduces their dynamics, promoting mitotic arrest and cell death. Paclitaxel, a representative anticancer agent of the taxanes, was initially defined by Horowitz and colleagues, and its binding sites are distinct from those of colchicine, podophyllotoxin, and the vinca alkaloids (7, 8). Paclitaxel initially received regulatory approval for the treatment of patients with ovarian cancer after failure of first-line or subsequent chemotherapy (9). In a Gynecologic Oncology Group study (GOG-111), it was thus determined to be the primary induction therapy in suboptimally debulked stage III and IV ovarian cancer, which mainly consists of serous adenocarcinoma (10). This study first compared the therapeutic efficacy of paclitaxel/cisplatin and cyclophosphamide/cisplatin in patients with ovarian cancer (10). The paclitaxel arm showed a distinct advantage in terms of progression-free survival (PFS) as well as overall survival (OS). A clinical trial by the European Organization for Research and Treatment of Cancer and the National Cancer Institute of Canada also showed that a paclitaxel/cisplatin regimen improved both PFS and OS (11). Another clinical trial study, however, reported that survival in the paclitaxel arm was similar to that seen in the control arm that received either carboplatin or cisplatin, doxorubicin, and cyclophosphamide (12). It remains unclear whether paclitaxel-cisplatin (or carboplatin) therapy is superior to cyclophosphamide/cisplatin (or carboplatin) therapy.

Of the various molecular markers related to drug sensitivity to taxanes, class III β-tubulin is expected to be a useful biomarker for the clinical efficacy of paclitaxel-based chemotherapy. Class III β-tubulin is hypothesized to counteract suppression of microtubule dynamics (13). Ferlini et al. reported that a novel taxane targeting class III β-tubulin overcame paclitaxel resistance, suggesting close involvement of this tubulin isotype in drug sensitivity to paclitaxel (14). Mozzetti et al. reported that class III β-tubulin overexpression represented a prominent mechanism of resistance to paclitaxel-platinum treatment in ovarian cancer (15). Moreover, class III β-tubulin overexpression could be useful in identifying poor clinical outcome in patients with advanced ovarian cancer who are treated with platinum/paclitaxel, those mainly affected with serous adenocarcinoma (16). These studies have been conducted mainly in serous adenocarcinoma of ovarian cancer. It remains unknown, however, whether class III β-tubulin overexpression is also predictive of poor outcome in clear cell adenocarcinoma, which is a rare variant in western countries, where it is reported to constitute 5% to 10% of ovarian carcinomas (17–19). Clear cell adenocarcinoma has been recognized as a chemoresistant phenotype (20, 21).

Japanese investigators have reported that clear cell adenocarcinoma constitutes about 20% of ovarian carcinomas in Japan (20, 22), although clear cell adenocarcinoma of the ovary accounts for only 2% to 5% of cases enrolled in large-scale randomized trials worldwide (22, 23). Thus, it is unclear whether carboplatin/paclitaxel therapy, which was introduced broadly as a standard regimen for epithelial ovarian cancer based on the results of such trials, can be readily applied for clear cell adenocarcinoma. Development of novel treatment strategies based on molecular biological characteristics is further required for clear cell adenocarcinoma.

In the present study, we addressed whether expression of β-tubulin III, MAP4, and stathmin could affect the efficacy of taxane-based therapeutic regimens against clear cell adenocarcinoma. Using immunohistochemical analysis of surgically resected clinical samples of clear cell adenocarcinoma, we examined expression levels of the above three biomarkers. In comparison with ovarian cancer patients treated with taxane-free regimens, we observed a significant and specific association of β-tubulin III expression with therapeutic outcomes of ovarian cancer treated with taxane-based regimens. We discuss whether the expression of β-tubulin III could be a predictive marker for the clinical efficacy of taxane-based chemotherapy against ovarian clear cell adenocarcinoma.

Materials and Methods

Cells and reagents. The human ovarian cell lines OVCAR-3 and SKOV-3, which expressed β-tubulins (I, II, III, and IV), MAP4, and stathmin, were obtained from the American Type Culture Collection. Cells were grown in Ham's F-12 Medium (Nissui Seiyaku Co.) with 10% fetal bovine serum (FetalClone III; Hyclone), 100 IU/mL penicillin, and 100 μg/mL streptomycin (Life Technologies, Inc.) in a humidified atmosphere of 5% CO_2 at 37°C. Paclitaxel (Taxol injection) and cisplatin (Briplatin injection) purchased from Bristol-Myers Squibb were clinically used. The polyclonal antistathmin was obtained from Calbiochem. The monoclonal class III β-tubulin antibody (clone 5G8) was obtained from Promega. The monoclonal MAP4 antibody (clone 18) was purchased from BD Transduction Laboratories.

Silencing of β-tubulins (I, II, III, IV), MAP4, and stathmin genes. To reduce the expression of some genes, we used Stealth RNAi (Invitrogen Life Technologies) to knock down the expression of β-tubulin I (NM_030773_stealth_706), β-tubulin II (NM_001069_stealth_1444), β-tubulin III (NM_006086_stealth_233), β-tubulin IV (NM_006087_stealth_352), MAP4 (NM_002375_stealth_2042), and stathmin (STMN1-HSS142799). Subconfluent human ovarian cells were cultured overnight in Opti-MEM I medium (Invitrogen Life

Technologies) without antibiotics, then 40 nmol/L small interfering RNA (siRNA) and Lipofectamine RNAiMax (Invitrogen) were applied according to the manufacturer's instructions. After 32 h, cells were detached from the culture plates and seeded into 96-well plates in F-12 medium with 10% fetal bovine serum. After a further 16-h incubation, paclitaxel or cisplatin was applied and cells were cultured for 3 d more. The numbers of cells were estimated by WST-8. The IC_{50} value was estimated from the regression line of log-logit plots of T/C (%) value versus drug concentration. The assays were carried out in quadruplicate.

Quantitative real-time PCR. RNA was reverse-transcribed from random hexamers using AMV reverse transcriptase (Promega). Real-time quantitative PCR was done using the Real-Time PCR system 7300 (Applied Biosystems). In brief, the PCR amplification reaction mixtures (20 μL) contained cDNA, primer pairs, the dual-labeled fluorogenic probe, and TaqMan Universal PCR Master Mix (Applied Biosystems). The thermal cycle conditions included maintaining the reactions at 50°C for 2 min and at 95°C for 10 min, and then alternating for 40 cycles between 95°C for 15 s and 60°C for 1 min. The primer pairs and probes were obtained from Applied Biosystems. The relative gene expression for each sample was determined using the formula $2^{(-\text{delta Ct})} = 2^{(\text{Ct (GAPDH)-Ct (target)})}$, which reflected the target gene expression normalized to GAPDH levels.

Patients. Ninety-four patients with primary ovarian clear cell adenocarcinoma, who had undergone debulking surgery at Keio University Hospital from 1983 to 2005, were examined. The histopathologic diagnoses of the all cases were confirmed according to the most recent WHO classification (WHO 2003). Patients were staged according to the International Federation of Obstetrics and Gynecology (FIGO) classification (24). Forty-four patients underwent chemotherapy using regimens containing taxanes [paclitaxel plus carboplatin (n = 39), paclitaxel plus cisplatin (n = 3), docetaxel plus cisplatin (n = 2); paclitaxel, 180 mg/m^2 body surface/day 1, docetaxel, 70 mg/m^2 body surface/day 1, cisplatin, 60 mg/m^2 body surface/day 1, and carboplatin, area under the curve 6/day 1]. Fifty patients received taxane-free regimens [CAP groups (n = 36): cisplatin (60 mg/m^2 body surface/day 1), epirubicin (50 mg/m2 body surface/day 1), and cyclophosphamide (500 mg/m^2 body surface/day 1); CAP plus fluorouracil (n = 1), CAP plus tegafur-uracil (n = 2), cisplatin plus cyclophosphamide (n = 11)]. The doses of carboplatin were calculated using Calvert's formula.

The effect of chemotherapy was evaluated approximately every 6 mo by computed tomography after 6 cycles of administration of chemotherapy. After chemotherapy, all patients were followed up every 2 mo for the first year, every 3 to 4 mo for the next 2 y, and every 6 mo

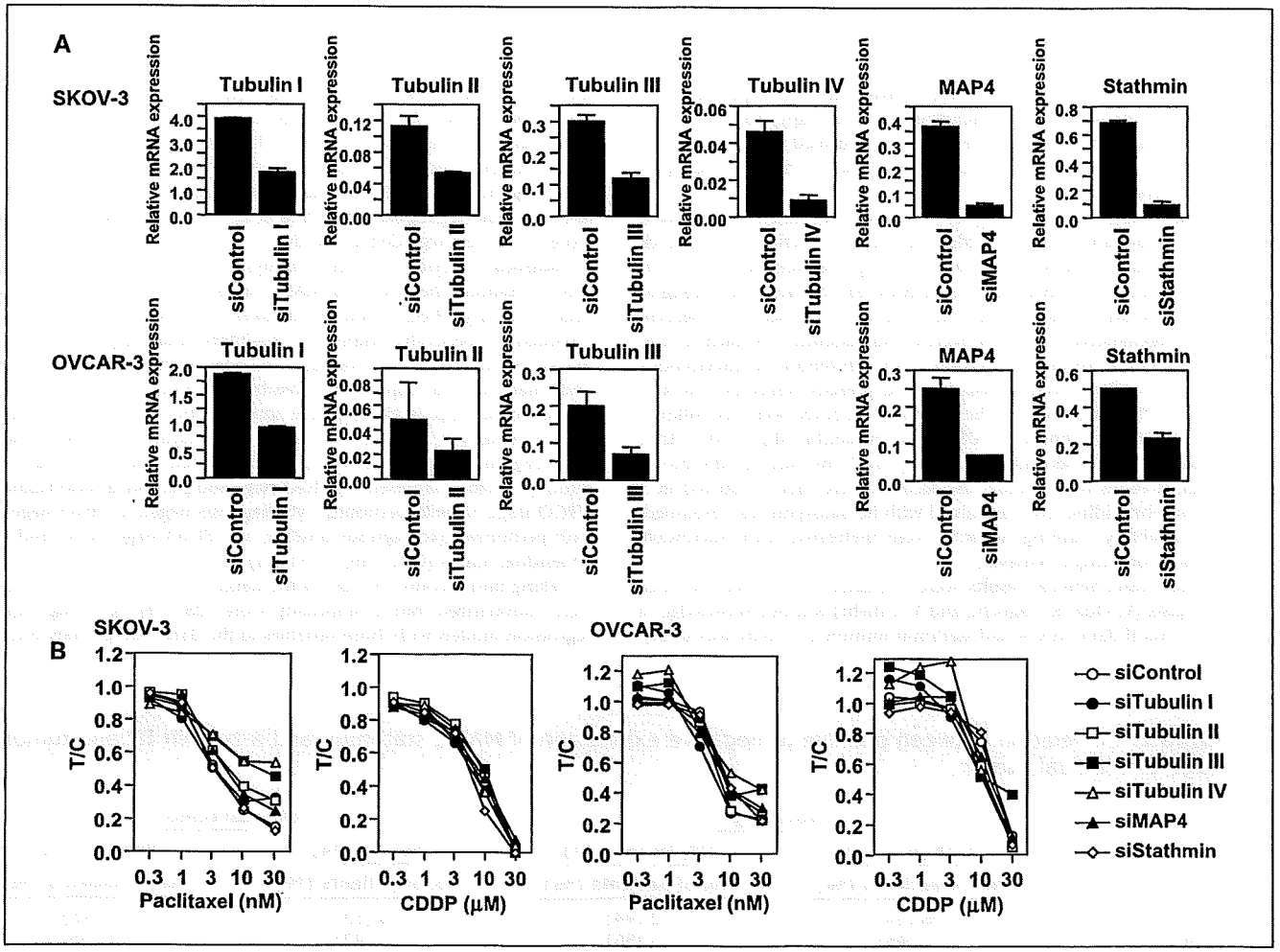

Fig. 1. Drug sensitivity to paclitaxel or cisplatin in human ovarian cancer cells treated with siRNA for β-tubulin isoforms, MAP4, and stathmin. *A*, mRNA expression of β-tubulin isoforms (I, II, III, IV), MAP4, and stathmin after treatment with respective siRNA for 48 h were determined by real-time PCR analysis. The expression of β-tubulin IV mRNA in OVCAR-3 cells was not detected. *B*, cells treated with respective siRNA were seeded into 96-well plates at 2 × 10^3 cells/0.1 mL/well and incubated overnight. On the following day, a 100-μL aliquot containing paclitaxel or cisplatin was added to the wells and cultured for a further 3 d. The number of viable cells was estimated using the WST-8 assay. The assays were carried out in quadruplicate.

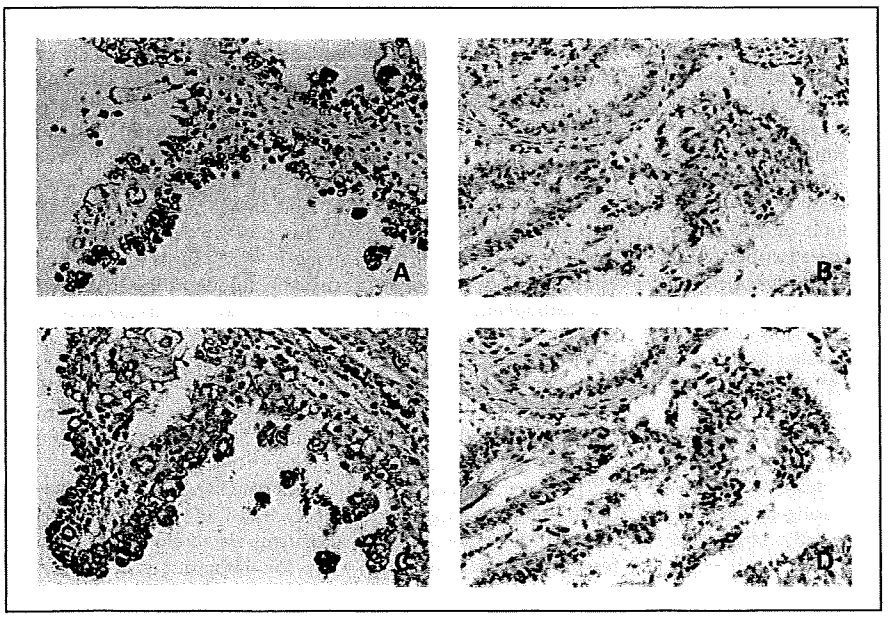

Fig. 2. *A* and *C*, stage IIc clear cell adenocarcinoma of a 55-year-old woman treated with the paclitaxel-carboplatin regimen. Cytoplasmic strong expression of stathmin (*A*, >15%) and β-tubulin III (*C*, score 7) can be diffusely observed in the tumor cells. The patient currently shows no evidence of disease 2,487 d (83 mo) after surgery. *B* and *D*, stage IIc tumor of a 56-year-old woman treated with the paclitaxel-carboplatin regimen. A few tumor cells (<15%) show only faint immunoreactivity for stathmin in the cytoplasm or nuclei, which was judged as negative (*C*). β-Tubulin III can be recognized in 10% of tumor cells with intermediate intensity and was interpreted as negative (score 4; *D*). This patient died of disease 447 d (15 mo) after initial surgery.

thereafter. Clinical outcome was measured by PFS and OS. PFS was defined as the interval from the date of first treatment (laparotomy or the first administration of neoadjuvant chemotherapy) to the date of the diagnosis of progression. We obtained informed consent from all patients, and personal information was removed from all samples before analysis.

Immunohistochemistry. Surgically resected specimens were fixed with 10% formalin and embedded in paraffin. Sections 4-μm thick on silane-coated slides were stained using the streptavidin-biotin-peroxidase method with a Histofine SAB-PO kit (Nichirei) according to the manufacturer's instructions. At least one representative section without degenerative change or necrosis was examined in each tumor. After deparaffinization, rehydration, and inhibition of endogenous peroxidase, sections were exposed to the primary antibodies at 4°C overnight. The dilutions of the primary antibody were as follows: MAP4, 1:1500; stathmin, 1:1000; and β-tubulin III, 1:200. After incubation of the secondary antibody and the streptavidin-biotin complex at room temperature, the sections were then incubated in 3 3'- diaminobenzidine, counterstained with hematoxylin, and mounted. For all antibody staining, sections were pretreated with microwave irradiation for antigen retrieval.

Immunohistochemical results were evaluated and scored by three pathologists (Y. Oda, K. Taguchi, and Y. Ohishi) without knowledge of patient clinical data. MAP4 and stathmin immunoreactivity was scored by estimating the percentage of labeled tumor cells. When >80% of the tumor cells showed immunoreactivity for MAP4, we judged the case to be positive. For stathmin expression, the cutoff value was 15%, based on a previous study (25). For class III β-tubulin expression, we evaluated the proportion and intensity of the immunoreactive cells following the protocol used to evaluate estrogen/progesterone receptors in breast cancer, proposed by Allred et al. (26, 27). Cases with a total score of ≥7 were regarded as positive.

Statistical analysis. Statistical analysis was conducted for OS and PFS to examine the effects of MAP4, stathmin, and β-tubulin III on taxane efficacy. Product-limit estimators of survival functions were obtained, respectively, relative to positivity and negativity of each marker in the patients to investigate the relationship between regimens and markers. To adjust for possible confounding factors, Cox proportional hazards models were applied. The covariates considered were a treatment indicator (0, taxane-free regimen; 1, taxane-based regimen), marker (0, negative; 1, positive), their interaction, age, two dummy variables representing FIGO stage and peritoneal cytodiagnosis (FIGO stage I-II with peritoneal cytodiagnosis negative, FIGO stage I-II with peritoneal cytodiagnosis positive, and FIGO stage III-IV) and size of residual tumor (0, <1 cm; 1, ≥1 cm).

Taking into account the size of the dataset, the latter four covariates were summarized into a propensity score (28, 29) by fitting logistic regression models with those variables to the data. The primary interest

Table 1. Correlation between positive or negative expression of MAP4, stathmin, and β-tubulin III and tumor stage or residual tumor

	FIGO stage		Residual tumor	
	I/II (*n* = 67)	III/IV (*n* = 27)	No (*n* = 74)	Yes (*n* = 20)
	No. of patients (%)	No. of patients (%)	No. of patients (%)	No. of patients (%)
MAP4 (-)	36 (54)	12 (44)	39 (53)	9 (45)
MAP4 (+)	31 (46)	15 (56)	35 (47)	11 (55)
Stathmin (-)	29 (43)	11 (41)	33 (45)	7 (35)
Stathmin (+)	38 (57)	16 (59)	41 (55)	13 (65)
β-tubulin III (-)	30 (45)	11 (41)	33 (45)	8 (40)
β-tubulin III (+)	37 (45)	16 (59)	41 (55)	12 (60)

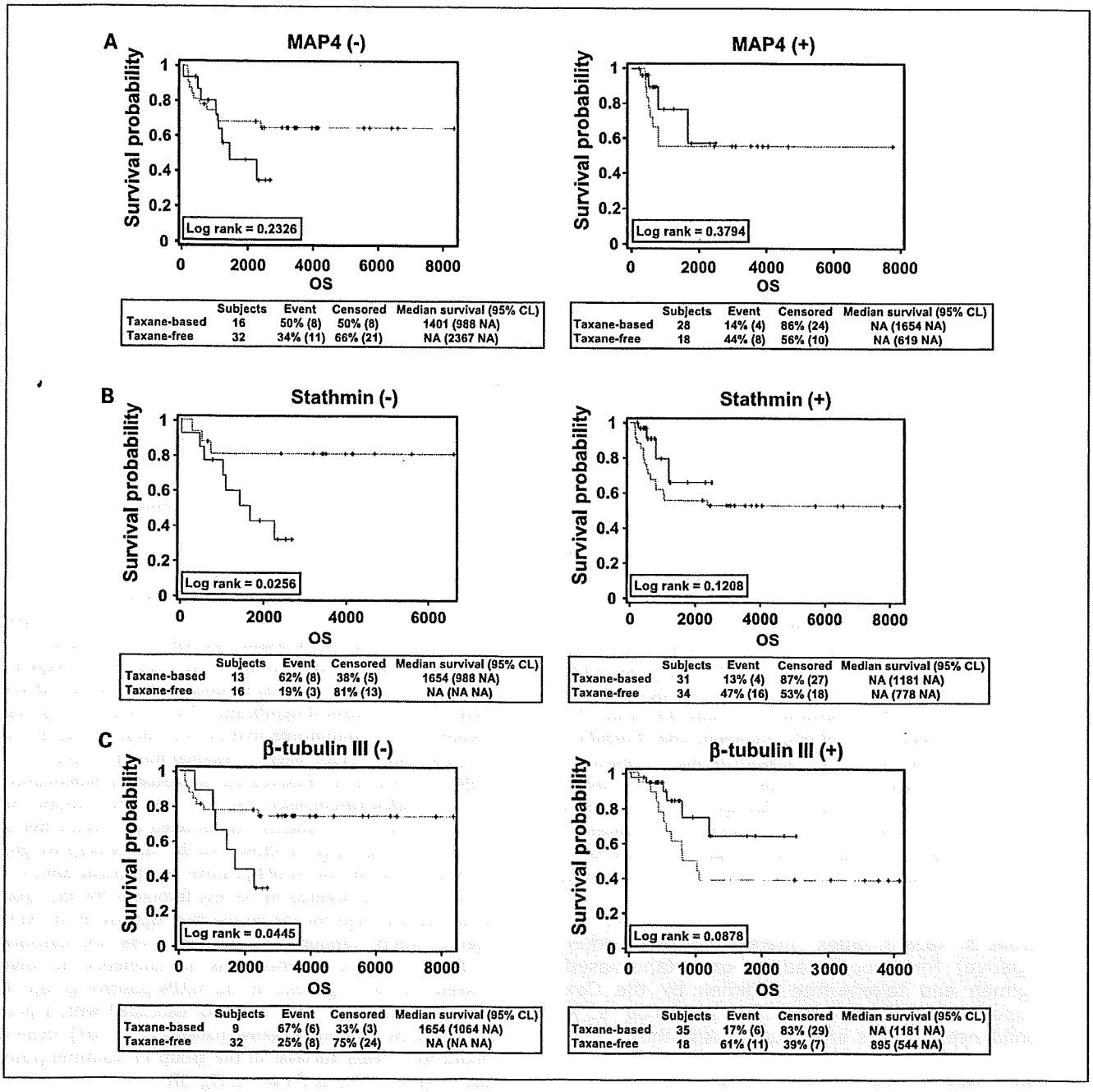

Fig. 3. The product-limit estimator of OS by regimens and microtubule-associated molecules. *A*, the product-limit estimators of OS for MAP4-negative patients (*left panel*) and for positive patients (*right panel*). *B*, the product-limit estimators of OS for stathmin-negative patients (*left panel*) and for positive patients (*right panel*). *C*, the product-limit estimators of OSfor β-tubulin III negative patients (*left panel*) and for positive patients (*right panel*). Solid lines, survival functions of patients receiving the taxane-based regimen; broken line, taxane-free regimen.

was the effect of the interaction between treatment and marker. With the supposition that the effect of a taxane-based regimen for marker-negative patients equals *A* and that of the taxane-free regimen for positive patients equals *B*, the significance of the interaction shows that the effect of the taxane-based regimen for the marker-positive patients is greater than *A+B* (i.e., it is synergistic). Evidence of a synergistic effect indicates that the effect of taxane is dependent on the status of the marker, showing the marker plays an important role in the effect of taxane. The cutoff points that determined positive and negative for each marker were chosen by the Akaike's information criterion so that the Cox model fitted best to the data (30).

Results

Effects of reducing expression of β-tubulin isoforms, MAP4, and stathmin on drug sensitivity to paclitaxel and cisplatin in ovarian cancer cells. We first examined whether gene silencing of

Table 2. Summary of interaction terms for the Cox regression

	MAP4	Stathmin	β-tubulin III
OS			
Regression coefficient (95% CI)	-0.77 (-2.50 to 0.96)	-1.37 (-3.17 to 0.43)	-1.68 (-3.16 to 0.21)
P	0.383	0.135	0.026
PFS			
Regression coefficient (95% CI)	-0.40 (-1.91 to 1.12)	-0.85 (-2.43 to 0.72)	-1.52 (-2.90 to -0.15)
P	0.608	0.288	0.030

Abbreviation: 95% CI, 95% confidence interval.

β-tubulin isoforms, MAP4, and stathmin could affect drug sensitivity to paclitaxel and cisplatin in the cultured human ovarian cancer cell lines SKOV-3 and OVCAR-3. Cellular mRNA expression levels of these genes in two human ovarian cancer cell lines were all markedly down-regulated when treated with respective siRNA (Fig. 1A). We then examined the drug sensitivities of paclitaxel or cisplatin in ovarian cancer cells treated with siRNA of the tubulin isoforms, MAP4, and stathmin (Fig. 1B). When β-tubulin III or β-tubulin IV was silenced, the IC_{50} values of paclitaxel increased to 16.8 nmol/L and 14.3 nmol/L, respectively, from the control IC_{50} value of 3.9 nmol/L in SKOV-3 cells (Fig. 1B). By contrast, down-regulation of β-tubulins I and II, MAP4, and stathmin did not influence the sensitivity to paclitaxel in SKOV-3 cells. Down-regulation of β-tubulins I, II, III, and IV, MAP4, and stathmin did not influence sensitivity to cisplatin in either cell line (Fig. 1B). Two independent experiments consistently showed the acquisition of drug resistance to paclitaxel in SKOV-3 by knockdown of β-tubulins III and IV.

Immunohistochemistry of MAP4, stathmin, and β-tubulin III in human ovarian clear cell adenocarcinomas. Clinical and pathologic characteristics at diagnosis are summarized in Supplementary Table S1. The median age of the patients was 52 years (range, 29-74 years). Sixty tumors were considered to be stage I, 7 stage II, 20 stage III, and 7 stage IV. Sixteen patients who had residual tumors more than 1 cm in maximum diameter were classified into the suboptimal group, whereas 78 patients were placed in the optimal group with a residual tumor ≤1 cm, including 74 complete resections. The median follow-up for PFS for all 94 patients was 749 days (range, 23-8,318 days), whereas the median follow-up for OS was 995 days (range, 23-8,318 days). The median follow-up of those patients who are currently progression-free is 2,399 days (range, 212-8,318 days).

The cytoplasmic positive expression of MAP4 was detected in 46 tumors (49%). Positive immunostaining for stathmin was found in 54 tumors (57%), predominantly as cytoplasmic staining (Fig. 2A). β-Tubulin III immunostaining was positive in 53 (56%) tumors with total scores of 7 or 8 (Fig. 2C). Positive MAP4 and β-tubulin III expression was frequent in tumors treated with taxane-containing regimens, compared with tumors treated with taxane-free regimens (Supplementary Table S1). Stathmin-positive tumors were also more frequent in patients with the taxane-based regimen, although the difference failed to reach statistical significance. There were no measurable differences in immunoreactivities for these proteins with respect to either tumor stage or residual tumor (Table 1).

Effects of β-tubulin III expression on survival in human ovarian clear cell adenocarcinomas. In Fig. 3A, the product-limit estimators for OS of patients administered the taxane-free and taxane-based regimens are shown for the MAP4-negative group (*left panel*) and for the MAP4-positive group (*right panel*). The survival outcome seemed to be less favorable for the taxane-based regimen than for the taxane-free regimen in the MAP4-negative group, although the difference was not statistically significant ($P = 0.23$); there was no difference in survival between the two regimens in the MAP4-positive group ($P = 0.38$). Paclitaxel treatment was also associated with a poorer survival in the stathmin-negative patients ($P = 0.03$); there was a trend to a better survival in the group of stathmin-positive patients ($P = 0.12$), as shown in Fig. 3B.

Survival associated with paclitaxel treatment was more evidently differential based on β-tubulin III status. In the absence of β-tubulin III expression, survival was significantly shorter in patients with the taxane-based regimen compared with those with the taxane-free regimen ($P = 0.04$), and the opposite was the case in the presence of β-tubulin III expression ($P = 0.09$; Fig. 3C). Table 2 gives the estimates, confidence intervals, and *P* values for the hazard ratios of the interaction. The table shows that for β-tubulin III, *P* values were 0.026 for OS and 0.030 for PFS. Thus, β-tubulin III seems to determine the efficacy of the taxane-based regimen. Table 2 also shows that for stathmin, *P* was 0.135 and the hazard ratio was 0.25 (95% confidence interval, 0.04-1.53) for OS, and 0.288 and 0.43, respectively (95% confidence interval, 0.09-2.06), for PFS.

Table 3. Hazard ratios (marker positive/marker negative) for subpopulations of taxane-based regimen and taxane-free regimen by the Cox proportional hazards models; two-tailed 95% confidence intervals are given in parenthesis

Marker hazard ratio (95% CI)	Taxane-based therapy	Taxane-free therapy	*P*
Overall survival			
MAP4	0.42 (0.11-1.66)	0.91 (0.35-2.40)	0.383
Stathmin	0.96 (0.26-3.53)	3.78 (1.07-13.34)	0.135
β-tubulin III	0.72 (0.22-2.44)	3.91 (1.49-10.23)	0.026
Progression-free survival			
MAP4	0.53 (0.17 -1.69)	0.79 (0.31-2.02)	0.608
Stathmin	1.11 (0.36-3.41)	2.60 (0.85-7.96)	0.288
β-tubulin III	0.77 (0.26-2.31)	3.52 (1.37-9.01)	0.030

NOTE: Age, FIGO stage, peritoneal cytodianosis, and size of residual tumor were adjusted by the propensity scores representing the four covariates.
P values are based on Wald tests for interaction of taxane with the marker.

Thus, stathmin may also determine the efficacy of the taxane-based regimen, but the effect was not statistically significant. Furthermore, Table 2 shows that for MAP4, the estimated hazard ratios were far from 1 but were not statistically significant (0.383 for OS and 0.673 for PFS).

The statistical significance of the interaction of taxane with β-tubulin III shown in Table 2 indicates that the efficacy of taxane depends on β-tubulin III positivity or negativity. To interpret this interaction precisely, we give the hazard ratio of the taxane-based regimen relative to the taxane-free regimen separately for β-tubulin III–positive and -negative patients. Table 3 gives the hazard ratios for patients who were positive for β-tubulin III relative to patients who were negative; these ratios are given separately for the taxane-based and taxane-free regimens. The table shows that the hazard ratio for OS was 3.91 for the taxane-free regimen but was 0.72 for the taxane-based regimen. This outcome indicates that being positive for β-tubulin III is related to a poor prognosis in the taxane-free regimen group, but that the taxane-based regimen may prolong OS for patients who are β-tubulin III–positive.

Discussion

Class III β-tubulin overexpression has been reported to be a marker of poor clinical outcome in patients with advanced ovarian cancer mainly containing serous type adenocarcinoma. With treatment using platinum/paclitaxel therapy (16), expression of class III β-tubulin also predicts response and outcome in patients with non–small cell lung cancer and in those with breast cancer who are treated with taxane-based chemotherapy (31, 32). In this study, we investigated which targets could be responsible for the therapeutic efficacy of taxane-based chemotherapy against ovarian clear cell adenocarcinoma patients when treated with either cisplatin/cyclophosphamide or cisplatin/taxane. Immunohistochemical staining was done for the surgically resected specimens using antibodies against class III β-tubulin, MAP4, and stathmin. Of these three targeting molecules, expression of class III β-tubulin was significantly associated with therapeutic efficacy of taxane-based chemotherapy, but not with taxane-free chemotherapy. Moreover, our present study showed that increased expression of class III β-tubulin significantly affected outcome for patients with ovarian clear cell adenocarcinoma in the taxane-treated patient group.

Our present finding is not consistent with those of previous studies identifying a close association of class III β-tubulin overexpression with poor therapeutic efficacy of taxane-based chemotherapy against ovarian cancers, including most non–clear cell adenocarcinomas (14–16). Of β-tubulin isoforms, microtubules containing tubulin III or IV were more dynamic and less stable than microtubules containing other tubulin types (13, 33), suggesting that cellular expression of β-tubulin isotype III or IV plays a critical role in drug sensitivity to paclitaxel *in vitro*. Paclitaxel-selected drug-resistant cancer cell lines derived from human lung, breast, pancreas, and prostate cancers and glioblastoma often exhibit enhanced expression of β-tubulin III (34). Kavallaris et al. have previously reported increased mRNA expression of β-tubulins III and IV in taxane-treated ovarian tumor samples as compared with primary untreated ovarian tumors (35). However, Nicolletti et al. have reported no correlation between tubulin expression and paclitaxel sensitivity in mouse xenografts of human ovarian carcinomas (36).

In our present study, knockdown of class III and IV β-tubulin genes but not of other tubulin isoforms specifically decreased drug sensitivity to paclitaxel in one ovarian cancer cell line, indicating the possible involvement of these tubulin isoforms in the dynamics of microtubules. At present, it remains unclear why decreased expression of type III β-tubulin differentially modulates drug sensitivity to paclitaxel among various cancer cell lines *in vitro*, and this finding requires further study. A complex network system among microtubule-related factors, including tubulin isoforms, operates in limiting drug sensitivity to taxanes; however, the results of our present study together with those of previous reports could present a novel notion that expression levels of class III β-tubulin might thus predict the therapeutic efficacy of taxane-based therapy. This effect would depend on differences in pathologic subtype between serous adenocarcinoma and clear cell adenocarcinoma.

We also found that OS of patients with lower expression of MAP4, stathmin, and β-tubulin indicated better therapeutic efficacy with non–taxane-based chemotherapy compared with taxane-based treatment. In patients with higher expression of stathmin and MAP4, these relationships were reversed but not statistically significant. Although these appeared during follow-up periods of the taxane-based therapy group for as long as 3,000 days, low expression of these three targeting molecules might predict poor prognosis for patients with ovarian clear cell adenocarcinoma.

Altered expression of proteins that regulate microtubule dynamics also mediates paclitaxel resistance in cancer cells *in vitro* through interaction with tubulin dimers or polymerizing microtubules. These proteins include stathmin, a microtubule destabilizer, and MAP4, a microtubule stabilizer (34). Altered expression of stathmin (5, 6) and MAP-4 (37) induces marked changes in drug sensitivity of cancer cells to taxanes. Further study is required to understand whether the above mechanisms *in vitro* underlie the poor therapeutic efficacy of taxane-based chemotherapy for patients with low expression of stathmin and MAP4, as well as β-tubulin. On the other hand, increased expression of stathmin also was associated (but not significantly) with an improved therapeutic efficacy of taxane-based chemotherapy in comparison with that of taxane-free therapy. Further study with a larger number of patients as well as longer follow-up periods may predict whether stathmin can be a marker for therapeutic efficacy of taxane-based therapy against ovarian clear cell adenocarcinoma.

In conclusion, our present study showed that overexpression of type III β-tubulin was a predictive marker of better prognosis for patients with ovarian clear cell adenocarcinoma when they are treated with taxane-based chemotherapy. This finding is not consistent with those involving patients with other serous type carcinoma treated by taxane-based chemotherapy, suggesting that association of β-tubulin expression with therapeutic efficacy by taxane-based chemotherapy depends on the pathologic characteristics of ovarian cancer.

Disclosure of Potential Conflicts of Interest

No potential conflicts of interest were disclosed.

References

1. Jordan MA. Mechanism of action of antitumor drugs that interact with microtubules and tubulin. Curr Med Chem Anti-Canc Agents 2002;2:1–17.
2. Drukman S, Kavallaris M. Microtubule alterations and resistance to tubulin-binding agents. Int J Oncol 2002; 21:621–8.
3. Maccioni RB, Cambiazo V. Role of microtubule-associated proteins in the control of microtubule assembly. Physiol Rev 1995;75:835–64.
4. Chapin SJ, Lue CM, Yu MT, Bulinski JC. Differential expression of alternatively spliced forms of MAP4: a repertoire of structurally different microtubule-binding domains. Biochemistry 1995;34:2289–301.
5. Balachandran R, Welsh MJ, Day BW. Altered levels and regulation of stathmin in paclitaxel-resistant ovarian cancer cells. Oncogene 2003;22:8924–30.
6. Alli E, Bash-Babula J, Yang JM, Hait WN. Effect of stathmin on the sensitivity to antimicrotubule drugs in human breast cancer. Cancer Res 2002;62: 6864–9.
7. Schiff PB, Fant J, Horwitz SB. Promotion of microtubule assembly *in vitro* by taxol. Nature 1979;277: 665–7.
8. Manfredi JJ, Parness J, Horwitz SB. Taxol binds to cellular microtubules. J Cell Biol 1982;94:688–96.
9. Rowinsky EK, Donehower RC. Paclitaxel (taxol). N Engl J Med 1995;332:1004–14.
10. McGuire WP, Hoskins WJ, Brady MF, et al. Cyclophosphamide and cisplatin compared with paclitaxel and cisplatin in patients in patients with stage III and stage IV ovarian cancer. N Engl J Med 1996;334:1–6.
11. Piccart MJ, Bertelsen K, James K, et al. Randomized intergroup trial of cisplatin-paclitaxel versus cisplatin-cyclophosphamide in women with advanced epithelial ovarian cancer: three-year results. J Natl Cancer Inst 2000;92:699–708.
12. International Collaborative Ovarian Neoplasm Group. Paclitaxel plus carboplatin versus standard chemotherapy with either single-agent carboplatin or cyclophosphamide, doxorubicin, and cisplatin in women with ovarian cancer: the ICON3 randomised trial. Lancet 2002;360:505–15.
13. Derry WB, Wilson L, Khan IA, Luduena RF, Jordan MA. Taxol differentially modulates the dynamics of microtubules assembled from unfractionated and purified β-tubulin isotypes. Biochemistry 1997;36: 3554–62.
14. Ferlini C, Raspaglio G, Mozzetti S, et al. The secotaxane IDN5390 is able to target class III β-tubulin and to overcome paclitaxel resistance. Cancer Res 2005;65:2397–405.
15. Mozzetti S, Ferlini C, Concolino P, et al. Class III β-tubulin overexpression is a prominent mechanism of paclitaxel resistance in ovarian cancer patients. Clin Cancer Res 2005;11:298–305.
16. Ferrandina G, Zannoni GF, Martinelli E, et al. Class III β-tubulin overexpression is a marker of poor clinical outcome in advanced ovarian cancer patients. Clin Cancer Res 2006;12:2774–9.
17. Scully RE. Tumors of the ovary and maldeveloped gonads. 3rd series. Washington (DC): Armed Forced Institute of Pathology; 1996. p. 141.
18. Seidman JD, Russell P, Kurman RJ. Surface epithelial tumors of the ovary. In: Blaustein A, Kurman RJ. Blaustein's pathology of the female genital tract. 5th ed. New York: Springer-Verlag; 2002. p. 873.
19. Shimizu M, Nikaido T, Toki T, Shiozawa T, Fujii S. Clear cell carcinoma has an expression pattern of cell cycle regulatory molecules that is unique among ovarian adenocarcinomas. Cancer 1999;85:669–77.
20. Ozols RF, Bundy BN, Greer BE, et al. Phase III trial of carboplatin and paclitaxel compared with cisplatin and paclitaxel in patients with optimally resected stage III ovarian cancer: a Gynecologic Oncology Group study. J Clin Oncol 2003;21:3194–200.
21. Sugiyama T, Kamura T, Kigawa J, et al. Clinical characteristics of clear cell carcinoma of the ovary. Cancer 2000;88:2584–9.
22. Pectasides D, Fountzilas G, Aravantinos G, et al. Advanced stage clear-cell epithelial ovarian cancer: the Hellenic Cooperative Oncology Group experience. Gynecol Oncol 2006;102:285–91.
23. du Bois A, Lück HJ, Meier W, et al. A randomized clinical trial of cisplatin/paclitaxel versus carboplatin/paclitaxel as first-line treatment of ovarian cancer. J Natl Cancer Inst 2003;95:1320–9.
24. International Federation of Gynecology and Obstetrics. Changes in definitions of clinical staging for cancer of the cervix and ovary. Am J Obstet Gynecol 1987;156:236–41.
25. Yuan RH, Jeng YM, Chen HL, et al. Stathmin overexpression cooperates with p53 mutation and osteopontin overexpression, and is associated with tumour progression, early recurrence, and poor prognosis in hepatocellular carcinoma. J Pathol 2006;209: 549–58.
26. Allred DC, Harvey JM, Berardo M, Clark GM. Prognostic and predictive factors in breast cancer by immunohistochemical analysis. Mod Pathol 1998;11: 155–68.
27. Ohishi Y, Oda Y, Basaki Y, et al. Expression of β-tubulin isotypes in human primary ovarian carcinoma. Gynecol Oncol 2007;105:586–92.
28. Rosenbaum PR, Rubin DB. The central role of the propensity score in observational studies for causal effects. Biometrika 1983;70:41–55.
29. Rosenbaum PR, Rubin DB. Reducing bias in observational studies using subclassification on the propensity score. J Am Stat Assoc 1984;79:516–24.
30. Akaike H. "A new look as the statistical model identification." IEEE Trans Autom Contr 1974;19:716–23.
31. Sève P, Mackey J, Isaac S, et al. Class III β-tubulin expression in tumor cells predicts response and outcome in patients with non-small cell lung cancer receiving paclitaxel. Mol Cancer Ther 2005;4:2001–7.
32. Paradiso A, Mangia A, Chiriatti A, et al. Biomarkers predictive for clinical efficacy of taxol-based chemotherapy in advanced breast cancer. Ann Oncol 2005; 16:14–9.
33. Panda D, Miller HP, Banerjee A, Luduena RF, Wilson L. Microtubule dynamics *in vitro* are regulated by the tubulin isotype composition. Proc Natl Acad Sci U S A 1994;91:11358–62.
34. Orr GA, Verdier-Pinard P, McDaid H, Horwitz SB. Mechanisms of Taxol resistance related to microtubules. Oncogene 2003;22:7280–95.
35. Kavallaris M, Kuo DY, Burkhart CA, et al. Taxol-resistant epithelial ovarian tumors are associated with altered expression of specific β-tubulin isotypes. J Clin Invest 1997;100:1282–93.
36. Nicoletti MI, Valoti G, Giannakakou P, et al. Expression of β-tubulin isotypes in human ovarian carcinoma xenografts and in a sub-panel of human cancer cell lines from the NCI-Anticancer Drug Screen: correlation with sensitivity to microtubule active agents. Clin Cancer Res 2001;7:2912–22.
37. Zhang CC, Yang JM, Bash-Babula J, et al. DNA damage increases sensitivity to vinca alkaloids and decreases sensitivity to taxanes through p53-dependent repression of microtubule-associated protein 4. Cancer Res 1999;59:3663–70.

Biochemical and Biophysical Research Communications 377 (2008) 826–831

Contents lists available at ScienceDirect

Biochemical and Biophysical Research Communications

journal homepage: www.elsevier.com/locate/ybbrc

Role of macrophages in inflammatory lymphangiogenesis: Enhanced production of vascular endothelial growth factor C and D through NF-κB activation ☆

Kosuke Watari [a,b], Shintaro Nakao [a], Abbas Fotovati [a], Yuji Basaki [a], Fumihito Hosoi [a], Biborka Bereczky [a], Ryuichi Higuchi [b], Tomofumi Miyamoto [b], Michihiko Kuwano [c], Mayumi Ono [a,*]

[a] Department of Pharmaceutical Oncology, Graduate School of Pharmaceutical Sciences, Kyushu University, Maidashi 3-1-1, Higashi-ku, Fukuoka 812-8582, Japan
[b] Department of Natural Products Chemistry, Graduate School of Pharmaceutical Sciences, Kyushu University, Fukuoka 812-8582, Japan
[c] Innovation Center for Medical Redox Navigation, Kyushu University, Fukuoka 812-8582, Japan

ARTICLE INFO

Article history:
Received 26 September 2008
Available online 23 October 2008

Keywords:
IL-1β
Lymphangiogenesis
Inflammation
VEGF-C
VEGF- D
VEGFR-3
Macrophage

ABSTRACT

The close association of inflammation, angiogenesis and cancer progression is now highlighted, and in this study we especially focused on a close association of inflammation and lymphangiogenesis. We found that proinflammatory cytokine, interleukin-1β (IL-1β), could induce lymphangiogenesis in mouse cornea through enhanced production of potent lymphangiogenic factors, VEGF-A, VEGF-C and VEGF-D. IL-1β-induced lymphangiogenesis, but not angiogenesis, was inhibited by administration of a selective anti-VEGF receptor-3 (VEGFR-3) neutralizing antibody. And in mouse cornea we observed recruitment of monocyte/macrophages and neutrophils by IL-1β implanted cornea. Depletion of macrophages by a bisphosphonate encapsulated in liposomes inhibited this IL-1β-induced lymphangiogenesis and also up-regulation of VEGF-A, VEGF-C, and VEGF-D. Furthermore, IL-1β-induced lymphangiogenesis and angiogenesis were suppressed by NF-κB inhibition with marked suppression of VEGF-A, VEGF-C, and VEGF-D expression.

Recently great progress has been made in understanding the mechanisms of lymphangiogenesis as a direct result of the discovery of a number of specific factors with essential roles in embryonic and postnatal lymphangiogenesis as well as pathological lymphangiogenesis. These lymphangiogenesis-related factors include prospero-related homeobox 1 (Prox-1), vascular endothelial growth factor C (VEGF-C), VEGF-D, vascular endothelial growth factor receptor-3 (VEGFR-3), lymphatic vessel endothelial hyaluronan receptor 1 (LYVE-1), podoplanin [1] and others. Of these, VEGF-C and VEGF-D are known to act as potent lymphangiogenesis factors by binding to their receptors, VEGFR-2 and VEGFR-3, both of which are expressed on LECs. Two other growth factors, VEGF-A and FGF-2, which are known to be potent angiogenic factors, also promote lymphangiogenesis [2,3]. FGF-2 has been shown to induce lymphangiogenesis in the mouse cornea via two pathways: first, by direct interaction with its cognate receptors on LECs; and second, by indirect activation of VEGF-C/VEGFR-3 signaling [4,5]. The development of novel lymphatic vessels is therefore regulated both by some factors that are common to angiogenesis, and by some factors that are specific for lymphangiogenesis.

The lymphatic vasculature plays an important role in the pathogenesis of human diseases such as cancer, lymphadenoma, and inflammatory disorders [1]. In particular, the development of novel lymphatic vessels is dependent upon Prox-1, VEGF-C, and VEGF-D expression and is closely associated with tumor metastasis [6]. Proinflammatory cytokines often enhance the expression of VEGF-C [7] as well as VEGF-A [8,9] during inflammation, and constitutively activate the transcription factor which typifies inflammation, nuclear factor-κB (NF-κB) [10]. Cursiefen et al. reported that VEGF-A-mediated lymphangiogenesis in inflamed corneas could be attributable to the recruitment of macrophages which produce VEGF-C and VEGF-D [2]. A study by Hamrah et al. showed that the expression of VEGF-C and its receptor VEGFR-3 is up-regulated in corneal dendritic cells after cauterization of the corneal surface in mice [11]. In mouse models of chronic respiratory tract inflammation, the growth of lymphatic vessels was found to be dependent upon VEGFR-3 signaling, but the growth of blood vessels was not [12]. In addition, dendritic cells, macrophages, neutrophils, and epithelial cells in the respiratory tract have been shown to express the VEGFR-3 ligands, VEGF-C and VEGF-D, which evoke lymphangiogenesis without hemangiogenesis [12]. These studies strongly suggest a relationship between

☆ *Acknowledgment of research support:* This research was supported by a grant-in-aid for Scientific Research for Priorify areas, Cancer, from the Ministry of Education Culture, Sports, Science and Technology of Japan (M.O.), and by the 3rd Term Comprehensive Control Research for Cancer from the Ministry of Health, Labor and Welfare, Japan (M.K.). This study was also supported in part by the Formation of Innovation Center for Fusion of Advanced Technologies, Kyushu University, Japan (M.O., M.K.).

* Corresponding author. Fax: +81 92 642 6296.
E-mail address: mono@phar.kyushu-u.ac.jp (M. Ono).

0006-291X/$ - see front matter © 2008 Elsevier Inc. All rights reserved.
doi:10.1016/j.bbrc.2008.10.077

lymphangiogenesis and the recruitment of leucocytes such as monocytes/macrophages and dendritic cells of monocytic lineage, to the cornea and other tissues undergoing inflammation.

Interleukin-1β (IL-1β) is a proinflammatory cytokine, and is the prototypical multifunctional cytokine that affects most cell types, often in accordance with other cytokines and low-molecular weight mediators [13]. IL-1β is present in the circulation of patients with a variety of diseases that involve infectious or inflammatory responses [14]. IL-1β and related inflammatory mediators enhance the expression of potent angiogenic factors such as interleukin-8 (IL-8) and VEGF-A resulting in the promotion of angiogenesis by both autocrine and paracrine mechanisms [8,9,15]. We previously reported that IL-1β could induce angiogenesis by enhancing the expression of prostanoids, CXC chemokines including IL-8, and VEGF-A, in the mouse cornea and in the tumor xenograft model of experimental angiogenesis [16,17]. Nakao and colleagues [18] have demonstrated that IL-1β-induced angiogenesis in mouse corneas is blocked by dexamethasone through its attenuation of NF-κB activating signaling. Ristimaki et al. have reported that IL-1β can also increase the expression of VEGF-C in human lung fibroblasts [7]. Although inflammation induced by corneal injury stimulates lymphangiogenesis [2,11,19], it remains unclear whether IL-1β itself can induce lymphangiogenesis.

In the present study, we examined the mechanism underlying the inflammatory cytokine IL-1β-induced lymphangiogenesis in mouse cornea. In addition, we considered the possible involvement of activated monocytes and macrophages in lymphangiogenesis in the response to inflammatory stimuli in corneas.

Materials and methods

Animals. All of the animal experiments were approved by the Committee on the Ethics of Animal Experiments at the Kyushu University, Japan. The male C57BL/6 mice, aged 6–10 weeks, were purchased from Kyudo (Saga, Japan).

Cells and reagents. Recombinant human IL-1β and FGF-2 were purchased from R&D Systems (Minneapolis, MN). Phosphatidylcholine, cholesterol, clodronate, and anti-α-SMA were purchased from Sigma-Aldrich (St Louis, MO). The NF-κB inhibitor SN50 was purchased from Biomol International (Plymouth Meeting, PA). Lymphatic endothelial cells (LECs) were purchased from Lonza Biologics Inc. (Portsmouth, NH) and cultured according to

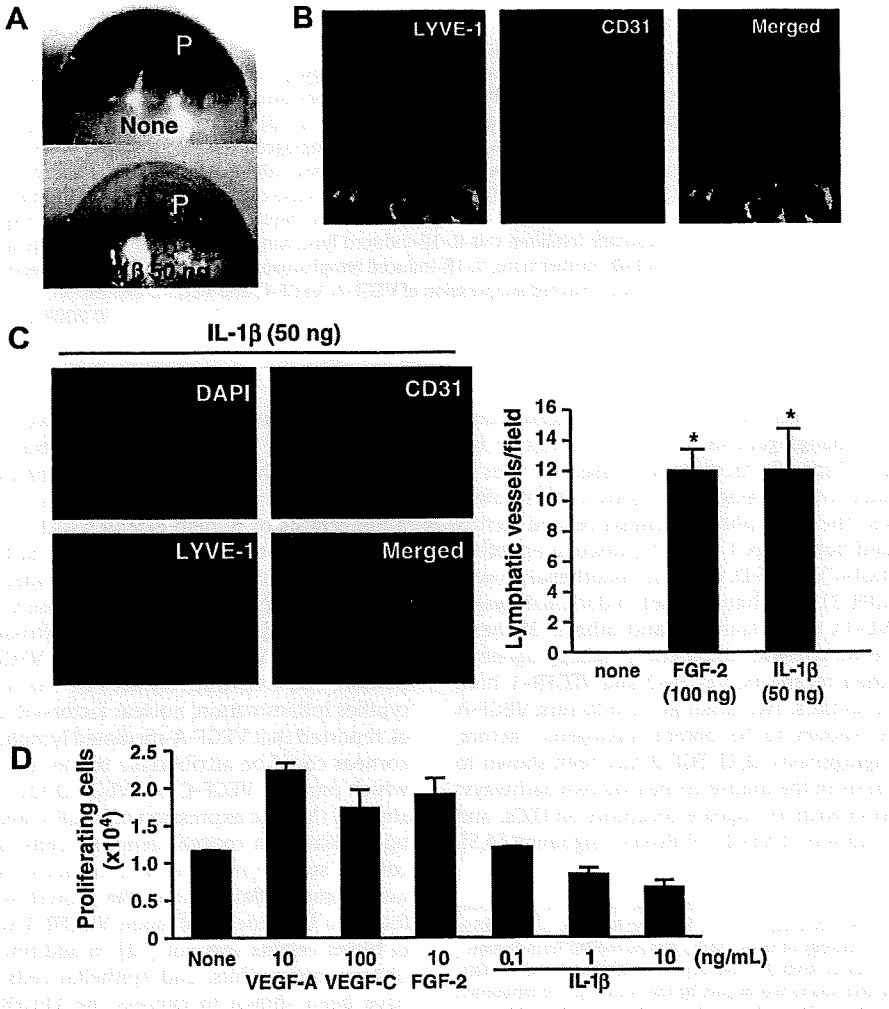

Fig. 1. Effect of IL-1β on corneal angiogenesis and lymphangiogenesis in mice. (A) Corneal neovascularization stimulated by implanted Hydron pellets (P) with or without 50 ng IL-1β was photographed 14 day later, in the region around the implants. (B) Whole corneal mount immunostained for LYVE-1 (green) and CD31 (red). (C) Immunostaining of LYVE-1 (green), CD31 (red), and DAPI (blue) in corneas treated with 50 ng IL-1β for 14 days. Quantification of lymphatic vessels in the corneas of mice treated with IL-1β and FGF-2. The number of lymphatic vessels was determined by scoring LYVE-1$^+$ vessels. The data represent the means ± SD. *Significant difference ($P < 0.01$). (D) Effect of VEGF-A, VEGF-C, VEGF-D, FGF-2, or IL-1β on LEC proliferation. The data represent the means ± SDs of triplicate dishes.

the manufacture's instructions. Anti-podoplanin was purchased from Angiobio (Del Mar, CA). PE-conjugated anti-mouse CD31 (PECAM-1) Ab was from BD Bioscience (San Jose, CA). Anti-F4/80 was from Serotec (Atlanta, GA). Anti-Gr-1 Ab was from Cayman Chemical Co. (Ann Arbor, MI),

Proliferation assay by LEC. The LECs were suspended in Eagle's basal medium 2 supplemented with 2% fetal bovine serum (FBS) and growth factors. After 2.5×10^4 cells were seeded in 24-well plates (IWAKI, Tokyo, Japan) and incubated for 24 h at 37 °C, the medium was changed to Eagle's basal medium 2 containing 0.5% FBS with VEGF-A, VEGF-C, FGF-2, or IL-1β in each well. After 48 h incubation, cell number in each well was counted.

Corneal micropocket assay in mice. A corneal micropocket assay was used to quantify corneal neovascularization in response to 0.3 μL Hydron pellets (IFN Sciences, NJ) containing 50 ng human IL-1β or human FGF-2, together with 500 ng rat anti-mouse VEGFR-3 antibody [20] in some cases, which were implanted in the corneas of the mice. The pellets were positioned 1 mm away from the corneal limbus. After 14 days, the corneal vessels were photographed and recorded using Viewfinder 3.0 (Pixera) with standardized illumination and contrast, and were then saved to disk. Liposome-encapsulated clodronate (Cl_2MDP-LIPs) was prepared as described previously [17]. Cl_2MDP-LIPs (200 μL) were injected intravenously and 10 μL Cl_2MDP-LIPs were injected subconjunctivally every other day. As a control, the same doses of PBS-LIPs were administered through the dual routs every other day. On the other hand, to examine the effect of a NF-κB inhibition using of NF-κB inhibitor, SN50 (25 μg/μL, 3 μL eye drops) were applied topically to IL-1β implanted eyes twice a day from day −1 to day 13. The quantitative analysis of neovascularization in the mouse corneas was performed using the National Institutes of Health image software package. Immunohistochemical staining and quantitative real-time PCR were performed as described previously [17].

Double-labeling whole mounts for LYVE-1 and CD31. The mouse eyes were enucleated on day 6 or 14 after implanting pellets containing IL-1β or FGF-2. The corneal tissue was dissected, fixed in cold 4% PFA for 1 h, and digested with 20 μg/mL proteinase K at 4 °C for overnight. The whole mounts were immunostained with a mixture of anti- LYVE-1 polyclonal Ab [21] and anti-CD31, followed by biotinylated anti-rabbit IgG (Vector Laboratories), as a secondary Ab, overnight at 4 °C. The Blood and lymphatic vessels were examined, and photographed under a Zeiss confocal microscope.

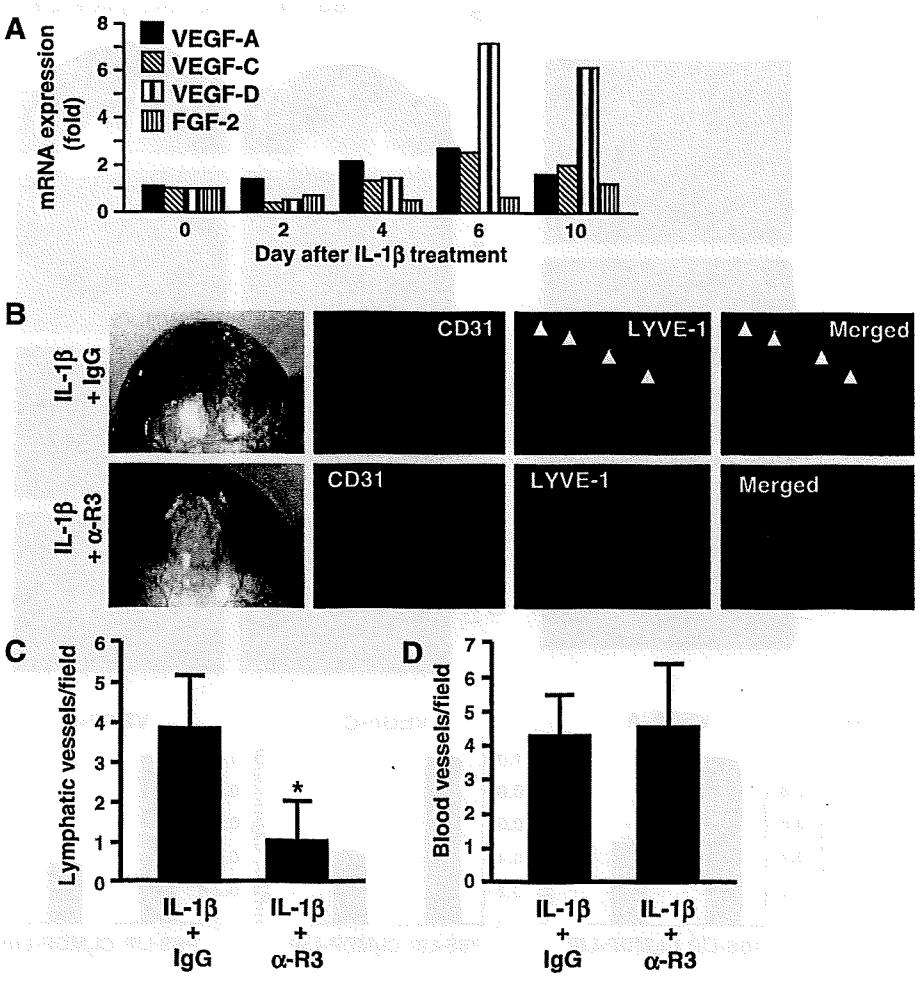

Fig. 2. Expression of VEGF family proteins and effect of neutralizing VEGFR-3 Ab on IL-1β-induced lymphangiogenesis. (A) Expression of VEGF-A, VEGF-C, VEGF-D, and FGF-2 in IL-1β-treated mouse corneas. The results shown were normalized to GAPDH mRNA levels and to corneal mRNA levels for each factor on day 0 (untreated control). Each value is the mean of six mice, and each mRNA level was within 5% of the mean value. (B) Hydron pellets containing 50 ng IL-1β with anti-VEGFR-3 Ab or control IgG Ab was implanted into the corneas of mice. After 14 days, frozen section of vessels were immunostained for LYVE-1 (green), CD31 (red), and DAPI (blue). (C) Quantification of lymphatic vessels and blood vessels by scoring LYVE-1$^+$ and CD31$^+$ vessels, respectively. All results are the means with the SDs ($n=5$). *Significant difference ($P<0.05$).

Results and discussion

IL-1β induces lymphangiogenesis as well as angiogenesis in mouse corneas, and the effect of VEGF-A, VEGF-C, FGF-2, and IL-1β on cell proliferation by LECs

In this study, we examined whether IL-1β could also induce lymphangiogenesis. The implantation of pellets containing 50 ng IL-1β induced neovascularization in the corneas of mice (Fig. 1A). Immunostaining whole mounts revealed the development of both LYVE-1$^+$ lymphatic vessels and CD31$^+$ blood vessels on day 14 after the implantation of pellets containing 50 ng IL-1β (Fig. 1B). Immunostaining of the corneal sections revealed the formation of both new lymphatic vessels and blood vessels (Fig. 1C). Quantification of the extent of lymphangiogenesis showed that 50 ng IL-1β induced new lymphatic vessels, and these numbers were comparable to those induced by 100 ng FGF-2 (Fig. 1C). By contrast, 10 ng IL-1β or 200 ng VEGF-A induced much less lymphatic vessels in the cornea (data not shown). These LYVE-1$^+$ vessels did not contain blood cells and did not express α-SMA, and most of these LYVE-1$^+$ vessels were also found to be positive for podoplanin, another lymphatic vessel specific marker (data not shown). We also observed LYVE-1$^+$ vessels in FGF-2-implanted corneas (Fig. 1C). We next examined whether IL-1β could directly stimulate angiogenic activity by looking its effects on proliferation and migration of LECs *in vitro*. LEC proliferation in culture was increased in response to exogenous VEGF-A, VEGF-C, and FGF-2, but was not affected by various doses of IL-1β (Fig. 1D). IL-1β at dose of 1 ng/mL was found to inhibit LEC proliferation (Fig. 1D), and IL-1β did not stimulate cell migration (data not shown).

Increased expression of VEGF family proteins in IL-1β-treated mouse corneas and inhibition of IL-1β-induced lymphangiogenesis by anti-VEGFR-3 antibody

We next examined the effect of IL-1β on the expression of the lymphangiogenesis-related factors VEGF-C, VEGF-D, and FGF-2, and the potent angiogenic factor, VEGF-A, in mouse cornea on day 0, 2, 4, 6, and 10. The VEGF-A, VEGF-C, and VEGF-D mRNA levels were increased with the time after IL-1β implantation in mice (Fig. 2A). The VEGF-A mRNA levels were markedly elevated on day 4 and followed a marked increase of VEGF-C and VEGF-D mRNA levels on day 6 and 10. VEGF-C and VEGF-D mediate their potent lymphangiogenic effects through their receptor, VEGFR-3, and neutralizing

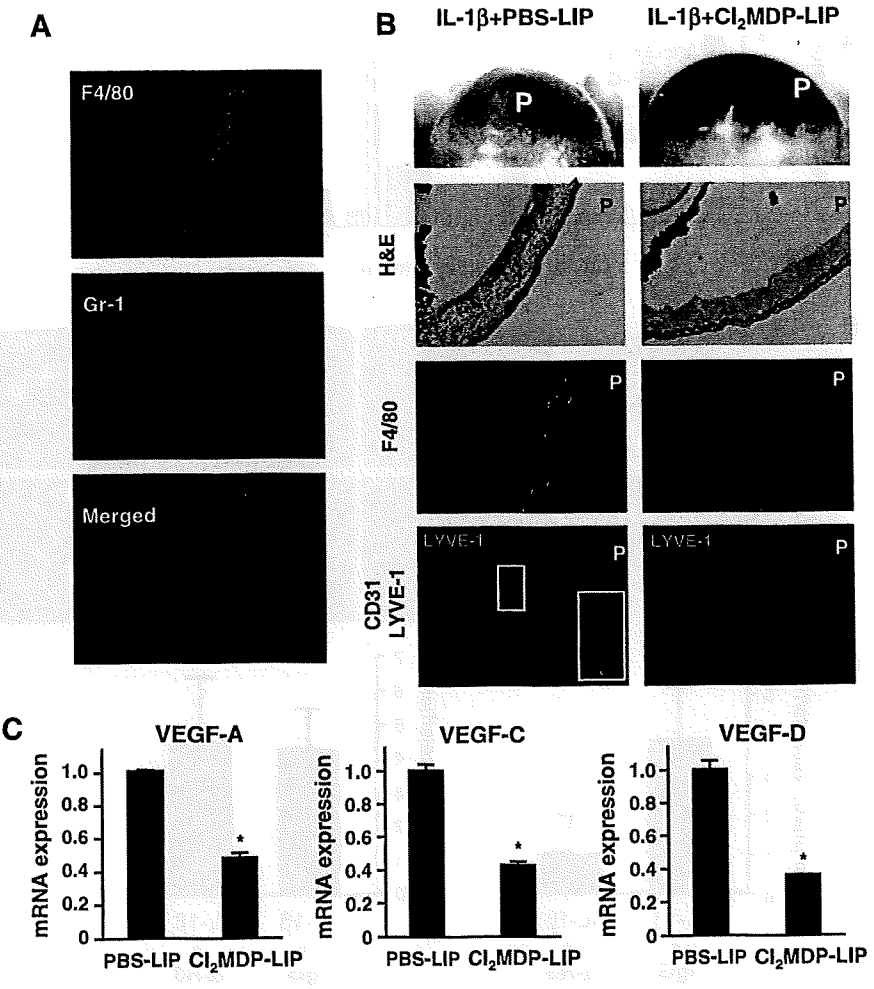

Fig. 3. Effect of macrophage depletion on IL-1β-induced lymphangiogenesis and mRNA expression of VEGF-A, VEGF-C, and VEGF-D. (A) Hydron pellets with or without 50 ng IL-1β were implanted into the corneas, and after 14 days, corneas were immunostained for monocyte/macrophages (F4/80, green), and neutrophils (Gr-1, red). (B) Hydron pellets (P) containing 50 ng IL-1β were implanted into the corneas of mice with or without administration of Cl_2MDP-LIP. After 14 days, vessels in the region of the pellet implants were immunostained for LYVE-1 (green), CD31 (red), DAPI (blue), and F4/80 (green). (C) Expression of VEGF-A, VEGF-C, and VEGF-D mRNAs in control and Cl_2MDP-LIP-treated corneas. Expression of VEGF family mRNAs was determined by quantitative RT-PCR. *Significant difference ($P<0.01$).

anti-VEGFR-3 Ab has been shown to selectively inhibit VEGF-C-induced lymphangiogenesis [22,23]. Treatment with anti-VEGFR-3 Ab (α-R3) had no apparent effect on IL-1β-induced angiogenesis, but inhibited the IL-1β-induced formation of LYVE-1$^+$ lymphatic vessels (Fig. 2B). Quantitative analysis demonstrated a significant ($P<0.05$) reduction in IL-1β-induced lymphangiogenesis by the α-R3 Ab (Fig. 2C). By contrast, α-R3 Ab did not affect the IL-1β-induced formation of CD31$^+$ vascular endothelial cells.

Effect of macrophage depletion on IL-1β-induced lymphangiogenesis and production of lymphangiogenic factors in vivo

Immunohistochemical analysis with the neutrophil-specific anti-Gr-1Ab and the macrophage-specific anti-F4/80 Ab revealed the infiltration of these inflammatory cells in IL-1β-induced lymphatic vessels and blood vessels in the cornea (Fig. 3A). We previously reported that IL-1β-induced angiogenesis in the mouse cornea was markedly suppressed when the macrophages in corneas and blood were depleted to 10–20% of the normal number by administration of Cl_2MDP-LIP via intravenous and subconjunctive injections [17]. Administration of Cl_2MDP-LIP markedly reduced the number of F4/80$^+$ macrophages in the cornea and also markedly inhibited angiogenesis (CD31$^+$ cells) and lymphangiogenesis (LYVE-1$^+$ cells) induced by IL-1β (Fig. 3B). Quantitative analysis demonstrated that mRNA levels of VEGF-A, VEGF-C, and VEGF-D in cornea were reduced by 50% or more in IL-1β-implanted mice only when the macrophages was depleted by Cl_2MDP-LIP (Fig. 3C). Taken together, macrophage depletion also affected the expression of VEGF-C, VEGF-D, and VEGF-A mRNA expression as well as lymphangiogenesis in IL-1β-treated corneas.

Effect of NF-κB inhibition on IL-1β-induced lymphangiogenesis and production of lymphangiogenic factors in vivo

To examine the role of NF-κB in the IL-1β-induced lymphangiogenesis and angiogenesis in the mouse corneas, we examined the effect of selective NF-κB inhibitor peptide, SN50. Typical examples of immunostaining whole mounts showed both LYVE-1$^+$ lymphatic vessels and CD31$^+$ blood vessels on day 14 after IL-1β implantation with or without SN50 (Fig. 4A). Quantitative analysis resulted in significant reduction of both angiogenesis and lymphangiogenesis by SN50 treatment in comparison with the untreated control group (Fig. 4B). Expression of VEGF-C and VEGF-D was markedly reduced to 20% or less in IL-1β-treated mice by SN50 as compared with control mice when those of VEGF-A mRNAs were reduced to about 50% (Fig. 4C). NF-κB activation thus might play a key role in the inflammatory cytokine-induced lymphangiogenesis and production of potent lymphangiogenic factors.

The activation of VEGFR-3 by its cognate ligands such as VEGF-C and VEGF-D has been reported to induce proliferation and migration by LEC [22]. Our *in vitro* study indicated that VEGF-A, VEGF-C, and FGF-2 stimulated proliferation and migration by LEC, but that IL-1β itself had no stimulatory effect on proliferation and

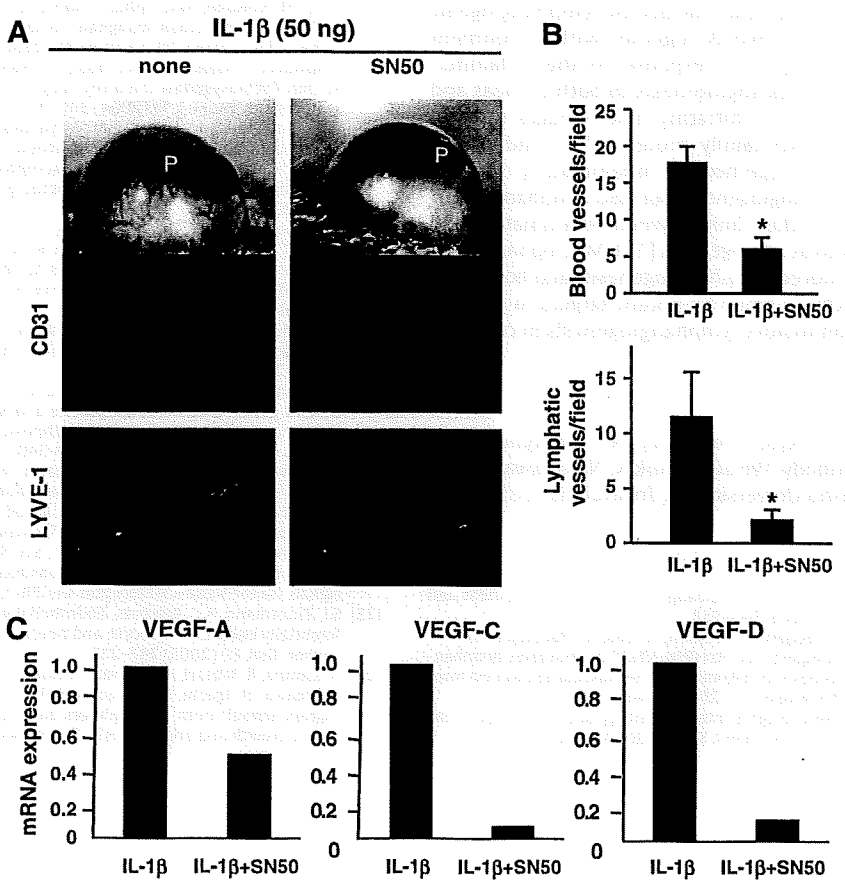

Fig. 4. Effect of NF-κB inhibition on IL-1β-induced corneal neovascularization and neolymphangiogenesis. (A) IL-1β-implanted corneas were topically treated with or without SN50. Immunostaining of CD31 (red) and LYVE-1 (green) in corneas treated with 50 ng IL-1β for 14 days with or without SN50. (P: pellet) (B) Quantification of blood vessels and lymphatic vessels in the corneas of mice treated with IL-1β in the absence or presence of SN50 for 14 days ($n=6$). (C) Expression of VEGF-A, VEGF-C, and VEGF-D mRNAs in untreated control and SN50-treated corneas. Expression of VEGF family mRNAs was determined by quantitative RT-PCR. *Significant difference ($P<0.05$).

migration. Furthermore, IL-1β-induced lymphangiogenesis was inhibited by simultaneous treatment with anti-VEGFR-3 Ab. IL-1β stimulated the expression of VEGF-A, VEGF-C, and VEGF-D, but not FGF-2, in cornea. As the interaction of VEGF-C and VEGF-D with VEGFR-3 selectively activates pro-lymphangiogenic signaling [1,6], IL-1β-induced lymphangiogenesis appears to be attributable to an indirect paracrine mechanism acting through VEGF-C/VEGF-D/VEGFR-3 signaling, rather than by a direct interaction with the IL-1β receptor.

IL-1β-induced inflammatory angiogenesis in mouse corneas was markedly blocked by a potent anti-inflammatory drug dexamethasone [18]. Dexamethasone inhibited NF-κB activation in corneal stromal cells, and treatment with a NF-κB inhibitory peptide SN50 markedly blocked the IL-1β-induced angiogenesis, suggesting NF-κB activating signaling was at least in part involved in the inflammatory cytokine-induced angiogenesis in corneas [18]. Consistent with this study, topical administration of SN50 blocked IL-1β-induced angiogenesis in corneas. Furthermore, administration of SN50 resulted in marked inhibition of both IL-1β-induced lymphangiogenesis and production of VEGF-C, VEGF-D, and VEGF-A (Fig. 4). Treatment of macrophages with IL-1β *in vitro* also enhanced production of VEGF-A and VEGF-D, and that this IL-1β-induced production of VEGF-A was blocked by a NF-κB inhibitor *in vitro* [24]. IL-1β-induced lymphangiogenesis as well as angiogenesis thus might be in part mediated by VEGF family proteins through activation of NF-κB, and favorably through NF-κB activated macrophages in corneal stroma.

In our present study, we have presented evidence that IL-1β can induce lymphangiogenesis in the mouse cornea, and that this activity is mediated by the up-regulation of potent lymphangiogenic factors VEGF-C, VEGF-D, and VEGF-A, together with recruitment and activation of macrophages in response to the inflammatory stimuli. IL-1β also induces angiogenesis in both corneas and tumors in mice, dependent on infiltrating macrophages through enhanced production of VEGF family proteins, IL-8 and matrix metalloproteases [13]. Taken together, the inflammatory cytokine IL-1β could induce not only angiogenesis but also lymphangiogenesis, supporting the idea of close link between inflammation and lymphangiogenesis as well as angiogenesis [13]. Macrophages play a key role in the IL-1β-induced lymphangiogenesis, and both macrophages and NF-κB pathway could be potent targets to develop drugs to control the inflammatory lymphangiogenesis in cancer.

Acknowledgments

We thank S. Nishikawa (Kyoto University) for supplying us rat anti-mouse VEGFR-3 antibody. We also thank K. Nakagawa, T. Nakano, and K. Sueishi (Kyushu University) for fruitful discussion.

References

[1] K. Alitaro, T. Tammela, T.V. Petrova, Lymphangiogenesis in development and human disease, Nature 438 (2005) 946–953.
[2] C. Cursiefen, L. Chen, L.P. Borges, D. Jackson, J. Cao, C. Radziejewski, P.A. D'Amore, M.R. Dana, S.J. Wiegand, J.W. Streilein, VEGF-A stimulates lymphangiogenesis and hemangiogenesis in inflammatory neovascularization via macrophage recruitment, J. Clin. Invest. 113 (2004) 1040–1050.
[3] S. Hirakawa, M. Detmar, New insights into the biology and pathology of the cutaneous lymphatic system, J. Dermatol. Sci. 35 (2004) 1–8.
[4] H. Kubo, R. Cao, E. Brakenhielm, T. Makinen, Y. Cao, K. Alitalo, Blockade of vascular endothelial growth factor receptor-3 signaling inhibits fibroblast growth factor-2-induced lymphangiogenesis in mouse cornea, Proc. Natl. Acad. Sci. USA 99 (2002) (2002) 8868–8873.
[5] L.K. Chang, G. Garcia-Cardena, F. Farnebo, M. Fannon, E.J. Chen, C. Butterfield, M.A. Moses, R.C. Mulligan, J. Folkman, A. Kaipainen, Dose-dependent response of FGF-2 for lymphangiogenesis, Proc. Natl. Acad. Sci. USA 101 (2004) 11658–11663.
[6] P. Saharinen, P.T. Tammela, M.J. Karkkainen, K. Alitalo, Lymphatic vasculature: development molecular regulation and role in tumor metastasis and inflammation, Trends Immunol. 25 (2004) 387–395.
[7] A. Ristimaki, K. Narko, B. Enholm, V. Joukov, K. Alitalo, Proinflammatory cytokines regulate expression of the lymphatic endothelial mitogen vascular endothelial growth factor-C, J. Biol. Chem. 273 (1998) 8413–8418.
[8] M. Ryuto, M. Ono, H. Izumi, S. Yoshida, H.A. Weich, K. Kohno, M. Kuwano, Induction of vascular endothelial growth factor by tumor necrosis factor-alpha in human glioma cells: possible roles of Sp-1, J. Biol. Chem. 271 (1996) 28220–28228.
[9] S. Yoshida, M. Ono, T. Shono, H. Izumi, T. Ishibashi, H. Suzuki, M. Kuwano, Involvement of interleukin-8, vascular endothelial growth factor, and basic fibroblast growth factor in tumor necrosis factor alpha-dependent angiogenesis, Mol. Cell. Biol. 17 (1997) 4015–4023.
[10] M.R. Saban, S. Memet, D.G. Jackson, J. Ash, A.A. Roig, A. Israel, R. Saban, Visualization of lymphatic vessels through NF-kappaB activity, Blood 104 (2004) 3228–3230.
[11] P. Hamrah, L. Chen, Q. Zhang, M.R. Dana, Novel expression of vascular endothelial growth factor (VEGFR-3) and VEGF-C on corneal dendritic cells, Am. J. Pathol. 163 (2003) 57–68.
[12] P. Baluk, T. Tammela, E. Ator, N. Lyubynska, M.G. Achen, D.J. Hicklin, M. Jeltsch, T.V. Petrova, B. Pytowski, S.A. Stacker, S. Yla-Herttuala, D.G. Jackson, K. Alitalo, D.M. McDonald, Pathogenesis of persistent lymphatic vessel hyperplasia in chronic airway inflammation, J. Clin. Invest. 115 (2005) 247–257.
[13] M. Ono, Molecular links between tumor angiogenesis and inflammation: inflammatory stimuli of macrophages and cancer cells as targets for therapeutic strategy, Cancer Sci. 99 (2008) 1501–1506.
[14] C.A. Dinarello, Biologic basis for interleukin-1 in disease, Blood 87 (1996) 2095–2147.
[15] H. Torisu, M. Ono, H. Kiryu, M. Furue, Y. Ohmoto, J. Nakayama, Y. Nishioka, S. Sone, M. Kuwano, Macrophage infiltration correlates with tumor stage and angiogenesis in human malignant melanoma: possible involvement of TNF alpha and IL-1 alpha, Int. J. Cancer 85 (2000) 182–188.
[16] T. Kuwano, S. Nakao, H. Yamamoto, M. Tsuneyoshi, T. Yamamoto, M. Kuwano, M. Ono, Cyclooxygenase 2 is a key enzyme for inflammatory cytokine induced angiogenesis, FASEB J. 18 (2004) 300–310.
[17] S. Nakao, T. Kuwano, C. Tsutsumi-Miyahara, S. Ueda, Y.N. Kimura, S. Hamano, K. Sonoda, Y. Saijo, T. Nukiwa, R.M. Strieter, T. Ishibashi, M. Kuwano, M. Ono, Infiltration of COX2-expressing macrophages is a prerequisite for IL-1β-induced neovascularization and tumor growth, J. Clin. Invest. 115 (2005) 2979–2991.
[18] S. Nakao, Y. Hata, M. Miura, K. Noda, Y. Kimura, Y.S. Kawahara, T. Kita, T. Hisatomi, T. Nakazawa, Y. Jin, R. Dana, M. Kuwano, M. Ono, T. Ishibashi, A. Hafezi-Moghadam, Dexamethasone inhibits IL-1β-induced corneal neovascularization: role of NF-κB-activated stromal cells in inflammatory angiogenesis, Am. J. Pathol. 171 (2007) 1058–1065.
[19] C. Cursiefen, L. Chen, M.R. Dana, J.W. Streilein, Corneal lymphangiogenesis: evidence, mechanisms, and implications for corneal transplant immunology, Cornea 22 (2003) 273–281.
[20] T. Nakano, Y. Nakanishi, Y. Yonemitsu, S. Sumiyoshi, Y.X. Chen, Y. Akishima, T. Ishii, M. Iida, K. Sueishi, Angiogenesis and lymphangiogenesis and expression of lymphangiogenic factors in the atherosclerotic intima of human coronary arteries, Hum. Pathol. 36 (2005) 330–340.
[21] K. Matsumura, M. Hirashima, M. Ogawa, H. Kubo, H. Hisatsune, N. Kondo, S. Nishikawa, T. Chiba, S. Nishikawa, Modulation of VEGFR-2-mediated endothelial-cell activity by VEGF-C/VEGFR-3, Blood 101 (2003) 1367–1374.
[22] T. Makinen, T. Veikkola, S. Mustjoki, T. Karpanen, B. Catimel, E.C. Nice, L. Wise, A. Mercer, H. Kowalski, D. Kerjaschki, S.A. Stacker, M.G. Achen, K. Alitalo, Isolated lymphatic endothelial cells transduce growth, survival and migratory signals via the VEGF-C/D receptor VEGFR-3, EMBO J. 20 (2001) 4762–4773.
[23] S.I. Zittermann, A.C. Issekuts, Endothelial growth factors VEGF and bFGF differentially enhance monocyte and neutrophil recruitment to inflammation, J. Leukoc. Biol. 80 (2006) 247–257.
[24] Y. Kimura, K. Watari, A. Fotovati, F. Hosoi, K. Yasumoto, H. Izumi, K. Kohno, K. Umezawa, H. Iguchi, K. Shirouzu, S. Takamori, M. Kuwano, M. Ono, Inflammatory stimuli from macrophages and cancer cells synergistically promote tumor growth and angiogenesis, Cancer Sci. 98 (2007) 2009–2018.

Molecular Basis for the Induction of an Angiogenesis Inhibitor, Thrombospondin-1, by 5-Fluorouracil

Hong-Ye Zhao,[1] Akio Ooyama,[3] Masatatsu Yamamoto,[1] Ryuji Ikeda,[1] Misako Haraguchi,[1] Sho Tabata,[1] Tatsuhiko Furukawa,[1] Xiao-Fang Che,[1] Shaoxuan Zhang,[1] Toshinori Oka,[3] Masakazu Fukushima,[3] Masayuki Nakagawa,[2] Mayumi Ono,[4] Michihiko Kuwano,[5] and Shin-ichi Akiyama[1]

[1]Department of Molecular Oncology and [2]Department of Urology, Graduate School of Medical and Dental Sciences, Kagoshima University, Sakuragaoka, Kagoshima, Japan; [3]Personalized Medication Research Laboratory, Taiho Pharmaceutical Company, Ebisuno, Tokushima, Japan; [4]Department of Pharmaceutical Oncology, Graduate School of Pharmaceutical Sciences, Kyushu University, Maidashi, Fukuoka, Japan; and [5]Innovation Center for Medical Redox Navigation, Kyushu University, Maidashi, Higashi-Ku Fukuoka, Japan

Abstract

5-Fluorouracil (5-FU) is one of the most commonly used anticancer drugs in chemotherapy against various solid tumors. 5-FU dose-dependently increased the expression levels of intrinsic antiangiogenic factor thrombospondin-1 (TSP-1) in human colon carcinoma KM12C cells and human breast cancer MCF7 cells. We investigated the molecular basis for the induction of TSP-1 by 5-FU in KM12C cells. Promoter assays showed that the region with the Egr-1 binding site is critical for the induction of *TSP-1* promoter activity by 5-FU. The binding of Egr-1 to the *TSP-1* promoter was increased in KM12C cells treated with 5-FU. Immunofluorescence staining revealed that 5-FU significantly increased the level of Egr-1 in the nuclei of KM12C cells. The suppression of Egr-1 expression by small interfering RNA decreased the expression level of TSP-1. Furthermore, 5-FU induced the phosphorylation of p38 mitogen-activated protein kinase (MAPK) and heat shock protein 27 (HSP27). Blockade of the p38 MAPK pathway by SB203580 remarkably inhibited the phosphorylation of HSP27 induced by 5-FU and decreased the induction of Egr-1 and *TSP-1* by 5-FU in KM12C cells. These findings suggest that the p38 MAPK pathway plays a crucial role in the induction of Egr-1 by 5-FU and that induced Egr-1 augments *TSP-1* promoter activity, with the subsequent production of TSP-1 mRNA and protein. [Cancer Res 2008;68(17):7035–41]

Introduction

5-Fluorouracil (5-FU) is a commonly used anticancer drug in chemotherapy against various solid tumors (1). Recent clinical studies have shown that UFT (a prodrug of 5-FU, Tegafur, combined with uracil in a 1:4 molar ratio) is an active oral chemotherapeutic agent in postoperative adjuvant settings for completely resected early-stage lung, gastric, colorectal, and breast cancer that does not exhibit any remarkable toxicity (2). UFT can achieve a higher maximum plasma 5-FU level for a longer period by inhibiting 5-FU degradation, thereby enhancing its antitumor effect (3). Angiogenesis is an important therapeutic target for a variety of malignant tumors. UFT-containing long-term chemotherapy significantly improved patient survival (4). The antiangiogenic effect of UFT might contribute, at least in part, to its clinical efficacy. Recently, we examined the antitumor and antiangiogenesis activities of the 5-FU–based drug, S-1 (1 mol/L teagaful, 0.4 mol/L 5-chloro-2,4-dihydroxypyridine, and 1mol/L potassium oxonate), at a sub–maximum tolerated dose (sub-MTD) on human colorectal cancer xenografts. The up-regulation of thrombospondin-1 (TSP-1), as well as down-regulation of microvessel formation, has been shown (5). However, the molecular basis for the suppression of angiogenesis by 5-FU has not been fully elucidated (6).

TSP-1 has been shown to inhibit angiogenesis by inhibiting endothelial cell migration, inducing endothelial cell apoptosis, directly interacting with vascular endothelial growth factor (VEGF), and inhibiting matrix metalloproteinase-9 activation (7). In addition, TSP-1 may inhibit angiogenesis by decreasing the level of circulating endothelial cell progenitors (8). However, the molecular basis for TSP-1 induction by 5-FU and other anticancer agents is unknown (9).

In the present study, we found that 5-FU induced TSP-1 in human colon carcinoma KM12C cells. A transcription factor, Egr-1, was also induced by 5-FU and bound to the promoter of *TSP-1*, enhancing its transcription and the subsequent production of TSP-1 protein. Moreover, we present the evidence that p38 mitogen-activated protein kinase (MAPK) plays an important role in 5-FU–induced Egr-1 transactivation.

Materials and Methods

Reagents and antibodies. 5-FU was provided by Taiho Pharmaceutical Co., Ltd. SB2003580 was obtained from Calbiochem. An antibody against Egr-1 was purchased from Santa Cruz Biotechnology. Mouse monoclonal antibodies against α-tubulin and TSP-1 were purchased from Oncogene and NeoMarkers, respectively. Anti–heat shock protein 27 (HSP27) G31 monoclonal and anti–phosphorylated HSP27 antibodies were obtained from Cell Signaling Technology.

Cell lines and cell cultures. KM12C human colon cancer cells were provided by Dr. Kiyoshi Morikawa (Iwamizawa Worker's Compensation Hospital), LOVO human colon cancer cells were purchased from Dainippon Seiyaku Co., Ltd., and MCF7 breast cancer cells were obtained from National Cancer Institute. The cells were grown in RPMI 1640 containing 10% heat-inactivated fetal bovine serum.

RNA isolation and cDNA synthesis. KM12C cells were treated with various concentrations of 5-FU for various periods, as described. The total RNA from the cultured cells were isolated using TRIzol (Invitrogen),

Note: Supplementary data for this article are available at Cancer Research Online (http://cancerres.aacrjournals.org/).

Requests for reprints: Shin-ichi Akiyama, Department of Molecular Oncology, Kagoshima University, Graduate School of Medical and Dental Sciences, 8-35-1 Sakuragaoka, Kagoshima 890-8544, Japan. Phone: 81-99-275-5490; Fax: 81-99-265-9687; E-mail: akiyamas@m3.kufm.kagoshima-u.ac.jp.

doi:10.1158/0008-5472.CAN-07-6496